SUPPORTING INFORMATION

Backbonding and non-covalent interactions in JohnPhos and polyfluorothiolate complexes of gold(I)

Guillermo Moreno-Alcántar[†], Kristopher Hess[†⁺], José Manuel Guevara-Vela[‡⁺], Tomás Rocha-Rinza[⸸], Angel Martín Pendás[‡], Marcos Flores-Álamo[†], Hugo Torrens[†]*.*

[†] Department of Inorganic and Nuclear Chemistry, School of Chemistry, UNAM, Ciudad Universitaria, 04510 CDMX, México. lgma@comunidad.unam.mx, torrens@unam.mx.

[‡]Department of Physical and Analytical Chemistry, University of Oviedo, Julián Clavería 8, Oviedo, Spain. E-33006.

[⸸]Department of Physical Chemistry, Institute of Chemistry, UNAM, Ciudad Universitaria, 04510 CDMX, México.

[⁺] These authors contribute equally.

Calculations concerning the C-S interaction

Table S1. QTAIM calculated parameters for the C-S interaction.

	C(para)-S		
Compound	$\rho(\mathbf{r}_{bcp})$	ε	DI
[Au(SC_6F_5)(JPhos)] 1	0.0053	0.8824	0.0282
[Au(SC_6HF_4)(JPhos)] 2	0.0055	0.8989	0.0276
[Au($SC_6H_3F_2$-3,5)(JPhos)] 3	0.0058	1.3781	0.0365
[Au($SC_6H_3F_2$-2,4)(JPhos)] 4	-	-	0.0012
[Au(SC_6H_4F-2)(JPhos)] 5	0.0062	1.6709	0.0341
[Au(SC_6H_4F-3)(JPhos)] 6	0.0057	0.1125	0.0360
[Au(SC_6H_4F-4)(JPhos)] 7	-	-	0.0255
[Au(SCF_3)(JPhos)] 8	0.0062	1.3340	0.0374

Note: There is no bond path for the C-S interaction in compounds 4 and 7 so $\rho(\mathbf{r}_{bcp})$ and ε could not be calculated. ε is very sensitive to integration errors due to the small electronic density values found for this interaction.

Crystallographic data

Table S2. Crystallographic data

	[Au(SC_6F_5)(JPh)]	**[Au(SC_6HF_4)(JPh)]**	**[Au($SC_6H_3F_2$-3,5)(JPh)]**	**[Au($SC_6H_3F_2$-2,4)(JPh)]**	**[Au(SC_6H_4F-2)(JPh)]**	**Au(SC_6H_4F-3)(JPh)]**	**Au(SC_6H_4F-4)(JPh)]**	**[Au(SCF_3)(JPh)]**
Empirical formula	C26 H27 Au F5 P S	C26 H28 Au F4 P S	C26 H30 Au F2 P S	C26 H30 Au F2 P S	C26 H31 Au F P S	C26 H31 Au F P S	C26 H31 Au F P S	C21 H27 Au F3 P S
Formula weight	694.47	676.48	640.49	640.49	622.50	622.50	622.50	596.42
Temperature	298(2) K	298(2) K	130(2) K	298(2) K	130(2) K	130(2) K	130(2) K	100(2) K
Wavelength	0.71073 Å	0.71073 Å	0.71073 Å	0.71073 Å	0.71073 Å	0.71073 Å	0.71073 Å	0.71073 Å
Crystal system	Orthorhombic	Orthorhombic	Triclinic	Monoclinic	Monoclinic	Triclinic	Triclinic	Monoclinic
Space group	P b c a	P b c a	P -1	P 21/n	P 21/c	P -1	P -1	P 21/n
Unit cell dimensions	a = 10.2791(4) Å	a = 10.3561(2) Å	a = 9.8864(6) Å	a = 13.3235(8) Å	a = 8.4347(8) Å	a = 11.0004(6) Å	a = 11.1857(4) Å	a = 10.4259(4) Å
	b = 19.2381(8) Å	b = 19.2100(5) Å	b = 11.9819(7) Å	b = 12.9471(6) Å	b = 17.9915(15) Å	b = 14.5902(6) Å	b = 14.4424(9) Å.	b = 18.4324(6) Å.
	c = 26.2618(10) Å	c = 25.7190(6) Å	c = 21.5082(11) Å	c = 15.1958(10) Å	c = 16.2240(13) Å	c = 16.9126(8) Å	c = 16.8674(10) Å	c = 11.9129(4) Å
			□= 75.206(5)°			□= 108.771(4)°	□□= 109.492(6)°	
			□= 82.287(5)°	□= 106.518(7)°.	□= 101.120(8)°	□= 104.898(4)°	□□= 104.940(4)°	□= 106.150(4)°
			□ = 85.619(5)°			□ = 91.213(4)°	□□ = 90.395(4)°.	
Volume	5193.3(4) $Å^3$	5116.6(2) $Å^3$	2438.7(2) $Å^3$	2513.1(3) $Å^3$	2415.8(4) $Å^3$	2467.6(2) $Å^3$	2468.9(2) $Å^3$	2199.01(14) $Å^3$
Z	8	8	4	4	4	4	4	4
Density (calculated)	1.776 Mg/m^3	1.756 Mg/m^3	1.744 Mg/m^3	1.693 Mg/m^3	1.712 Mg/m^3	1.676 Mg/m^3	1.675 Mg/m^3	1.802 Mg/m^3
Absorption coefficient	5.856 mm^{-1}	5.936 mm^{-1}	6.210 mm^{-1}	6.026 mm^{-1}	6.261 mm^{-1}	6.129 mm^{-1}	6.126 mm^{-1}	6.886 mm^{-1}
F(000)	2704	2640	1256	1256	1224	1224	1224	1160

Theta range for data collection	3.682 to 29.496°.	3.730 to 29.624°.	3.410 to 29.447°.	3.444 to 29.329°.	3.418 to 29.503°.	3.428 to 29.496°.	3.445 to 29.575°.	3.561 to 29.336°.
Index ranges	-13<=h<=10, -22<=k<=26, -36<=l<=24	-14<=h<=14, -25<=k<=24, -32<=l<=33	-13<=h<=13, -16<=k<=16, -27<=l<=29	-18<=h<=17, -17<=k<=12, -11<=l<=20	-11<=h<=11, -24<=k<=24, -20<=l<=20	-14<=h<=15, -20<=k<=19, -21<=l<=21	-14<=h<=15, -19<=k<=19, -23<=l<=20	-10<=h<=13, -15<=k<=25, -15<=l<=14
Reflections collected	17607	42047	21726	13387	25924	32793	27603	11088
Independent reflections	6213 [R(int) = 0.0492]	6643 [R(int) = 0.0328]	11357 [R(int) = 0.0433]	5974 [R(int) = 0.0343]	6060 [R(int) = 0.0575]	11912 [R(int) = 0.0488]	11810 [R(int) = 0.0365]	5159 [R(int) = 0.0441]
Completeness to theta = 25.242°	99.7 %	99.7 %	99.7 %	99.7 %	99.7 %	99.7 %	99.8 %	99.7 %
Refinement method	Full-matrix least-squares on F^2	Full-matrix least-squares on F^2	Full-matrix least-squares on F^2	Full-matrix least-squares on F^2	Full-matrix least-squares on F^2	Full-matrix least-squares on F^2	Full-matrix least-squares on F^2	Full-matrix least-squares on F^2
Data / restraints / parameters	6213 / 0 / 313	6643 / 0 / 304	11357 / 0 / 571	5974 / 0 / 286	6060 / 0 / 277	11912 / 0 / 553	11810 / 0 / 553	5159 / 0 / 250
Goodness-of-fit on F^2	1.077	1.076	0.972	1.029	1.056	1.064	1.055	1.117
Final R indices [I>2sigma(I)]	R1 = 0.0480, wR2 = 0.0795	R1 = 0.0322, wR2 = 0.0586	R1 = 0.0343, wR2 = 0.0580	R1 = 0.0346, wR2 = 0.0551	R1 = 0.0335, wR2 = 0.0764	R1 = 0.0338, wR2 = 0.0686	R1 = 0.0294, wR2 = 0.0495	R1 = 0.0356, wR2 = 0.0748
R indices (all data)	R1 = 0.0890, wR2 = 0.0921	R1 = 0.0551, wR2 = 0.0658	R1 = 0.0497, wR2 = 0.0646	R1 = 0.0699, wR2 = 0.0667	R1 = 0.0425, wR2 = 0.0829	R1 = 0.0470, wR2 = 0.0765	R1 = 0.0430, wR2 = 0.0546	R1 = 0.0457, wR2 = 0.0798
Extinction coefficient	n/a	n/a	n/a	n/a	n/a	n/a	n/a	n/a
Largest diff. peak and hole	0.966 and -1.585 e.Å^{-3}	0.880 and -0.798 e.Å^{-3}	1.058 and -1.868 e.Å^{-3}	0.645 and -0.655 e.Å^{-3}	1.673 and -1.847 e.Å^{-3}	1.320 and -1.925 e.Å^{-3}	0.830 and -1.012 e.Å^{-3}	1.937 and -1.358 e.Å-3

Theoretical-experimental correlations

^{31}P NMR and DI

As expected, the $^{31}P\{^{1}H\}$ NMR spectra of all 8 compounds examined exhibit a single resonance signal. One of the aims of this work was to explore the relationship of the corresponding chemical shift $\delta\ ^{31}P$ with the group electronegativity of the fluorinated thiols to assess the different *trans* effect of each ligand which is ultimately due to the electronegativity of the F atom. A more fluorinated thiolate is expected to attract more electrons from the S-Au-P system by decreasing the σ basicity of sulphur. This situation gives place to an unshielded phosphorus atom in *trans* position. Unfortunately, compounds **1**-**5** and **8** have practically the same value of chemical shifts, whereas compounds **6** [Au(SC_6H_4F-3)(JPhos)] and **7** [Au(SC_6H_4F-4)(JPhos)], present two larger values of δ. Since NMR cannot give us detailed information on the difference in chemical bonding in these compounds, we decided to use quantum chemical topology to get insights about this issue as reported in the main body of the paper.

Table S3. 31P chemical shifts for the compounds addressed in this investigation

Number	Compound	$\delta\ ^{31}P$ (ppm)
1	[Au(SC_6F_5)(JPhos)]	62.88
2	[Au(SC_6HF_4)(JPhos)]	62.83
3	[Au($SC_6H_3F_2$-3,5)(JPhos)]	63.48
4	[Au($SC_6H_3F_2$-2,4)(JPhos)]	63.08
5	[Au(SC_6H_4F-2)(JPhos)]	63.16
6	[Au(SC_6H_4F-3)(JPhos)]	68.31
7	[Au(SC_6H_4F-4)(JPhos)]	68.59
8	[Au(SCF_3)(JPhos)]	61.75

As stated in the manuscript, variations in the Au-S delocalization index are small, but it is still interesting to observe the relation between ^{31}P-NMR chemical shift and the DI between gold and sulphur (reported Table 1) that is shown in Figure S1. This relation establishes the trans influence tendencies of these thiolate ligands, i.e. the larger the electronic density in the Au-S fragment, the larger the unshielding of the trans phosphorus atom.

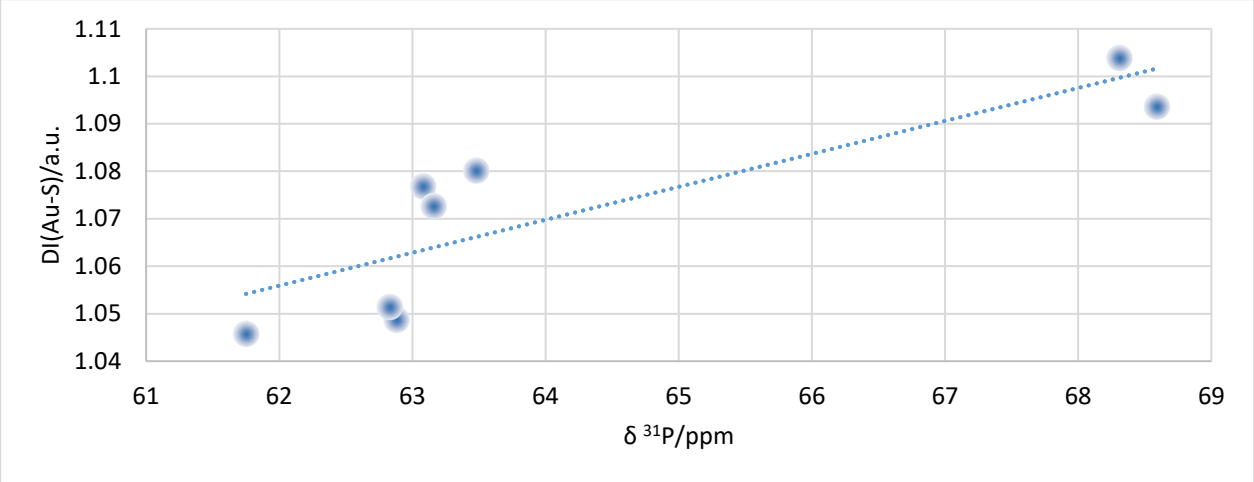

Figure S1. Relation between the delocalization index between the gold and the sulphur atom and the chemical shift of ^{31}P.

Au-C distance and p-backdonation

The Au-C distance and the Au-S ellipticity present a good correlation for the three monofluorinated compounds. This could mean that a larger π electronic density in the Au-S bond is related to a weaker Au-C interaction. Unfortunately, this trend is not clear for the other compounds probably due to packing and competence of other weak contacts.

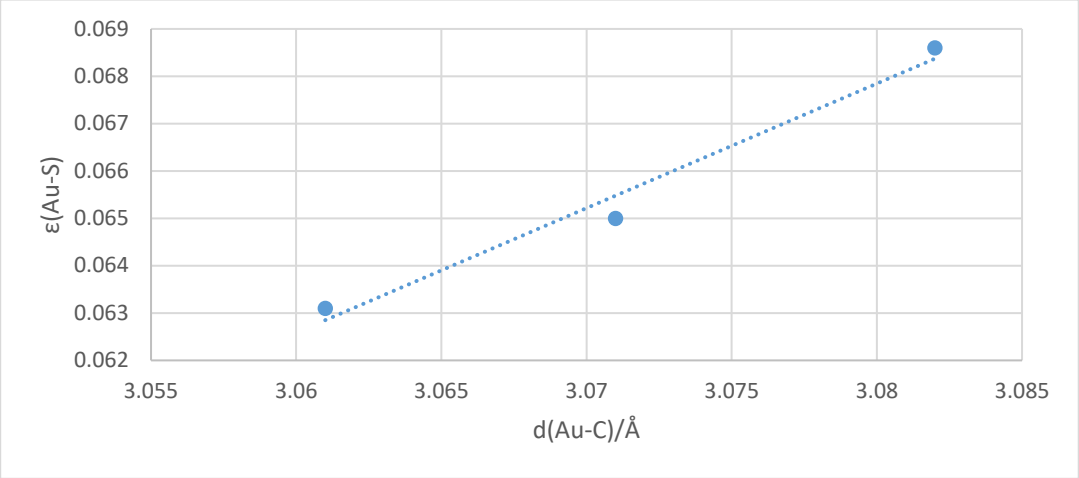

Figure S2. Relation between the ellipticity of the Au-S bond critical point and the Au-π interaction distance.

NMR Spectra.

Nuclear magnetic resonance spectra, ^{1}H-NMR, ^{13}C, ^{19}F and ^{31}P{^{1}H}, were recorded on a 9.4 T Varian VNMRS spectrometer. Chemical shifts are in ppm relative to internal TMS $\delta = 0$ (^{1}H, ^{13}C) and to external references of $CFCl_3$ (for ^{19}F) and H_3PO_4 (for ^{31}P) at 0 ppm. All spectra were obtained using acetone-d_6 as solvent at 25 °C.
Note 1: ^{1}H-NMR spectra display three signals corresponding to solvent, DHO and H_2O between 1.8 and 2.6 ppm

Compound 1. [Au(SC_6F_5)($PC_{20}H_{27}$)].
^{1}H-NMR

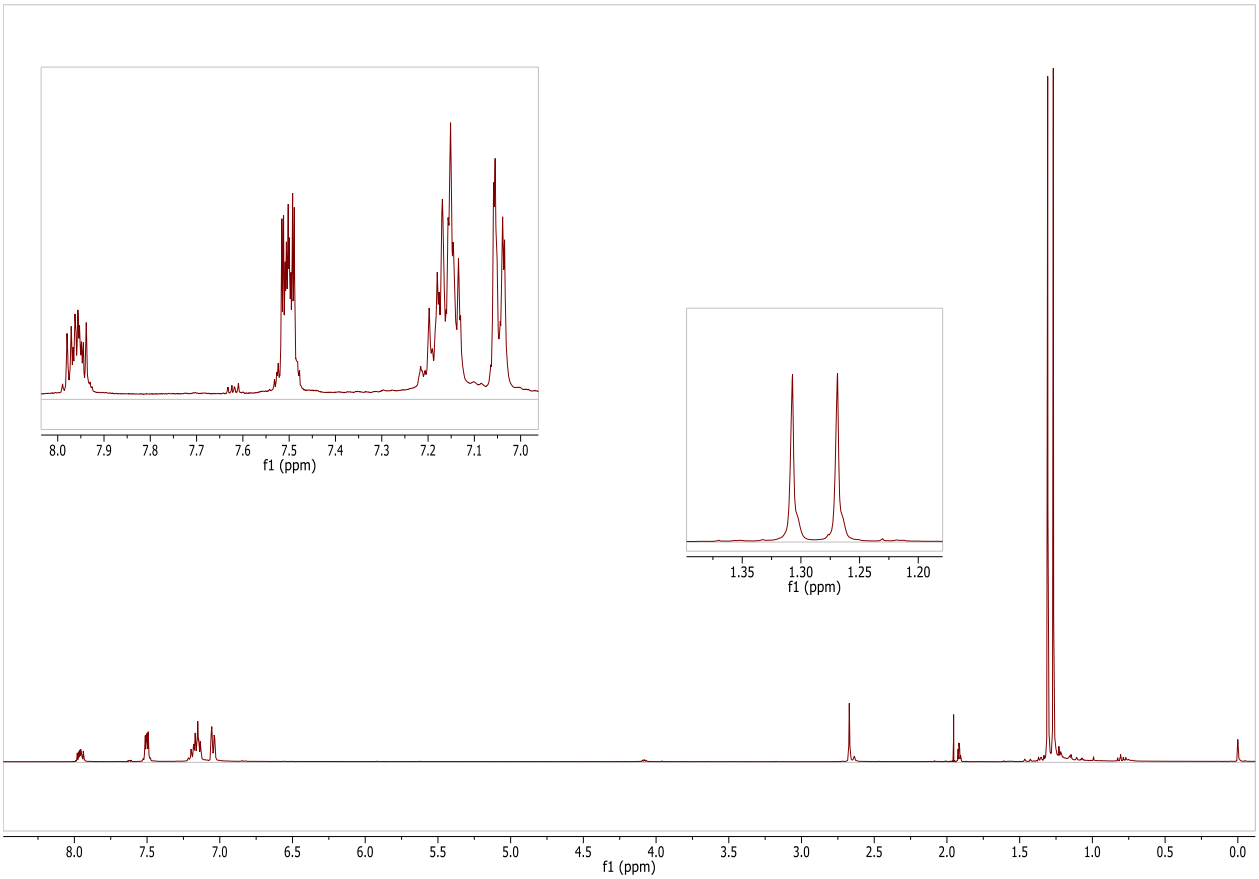

^{19}F-NMR

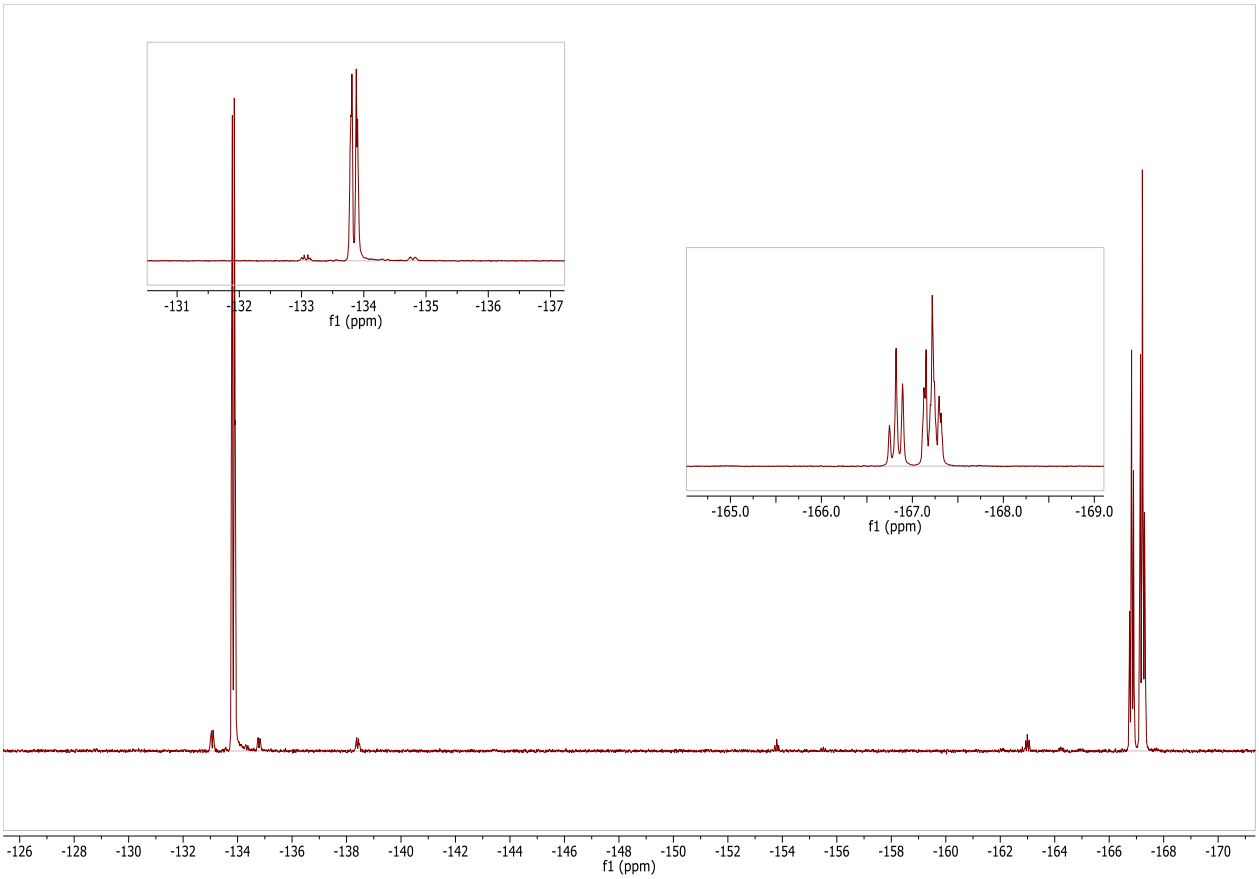

^{13}C-NMR

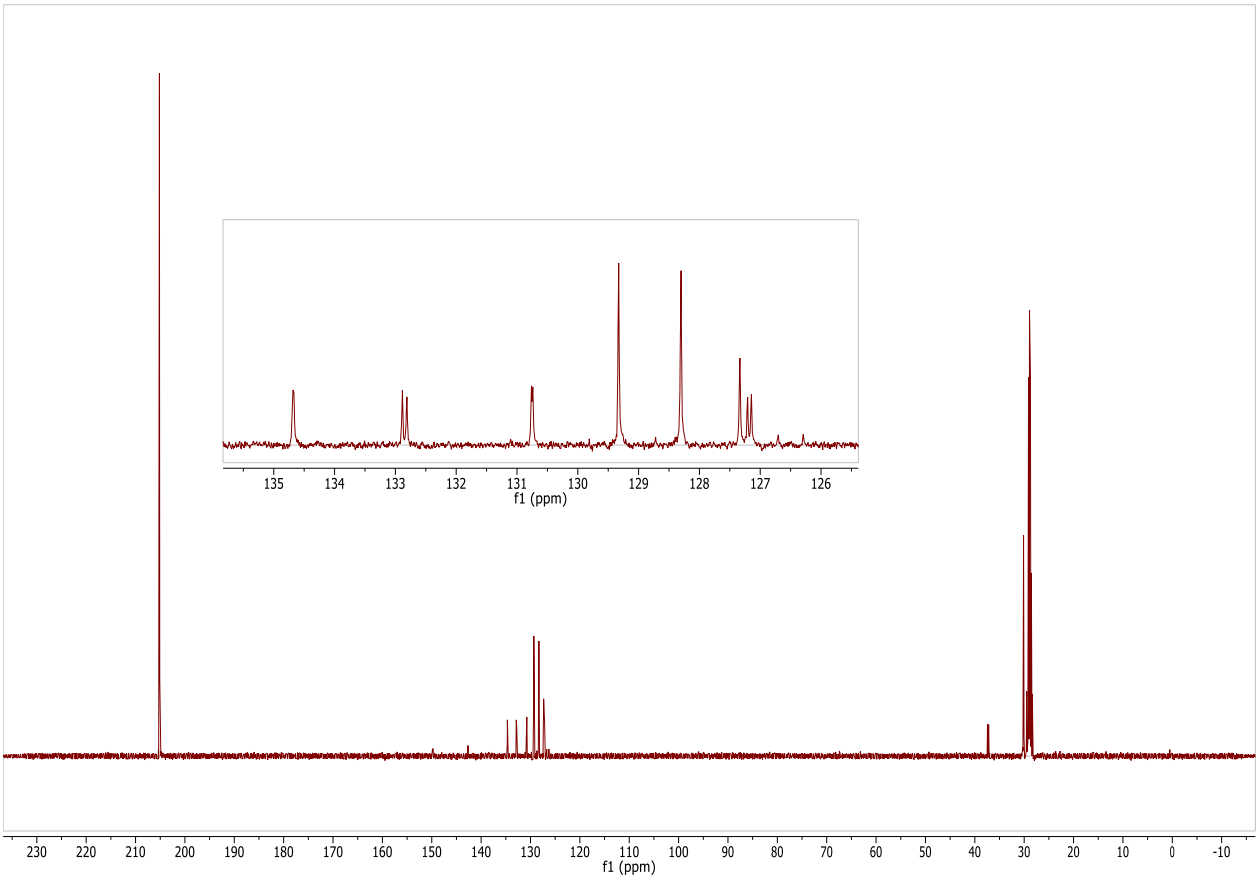

^{31}P-NMR

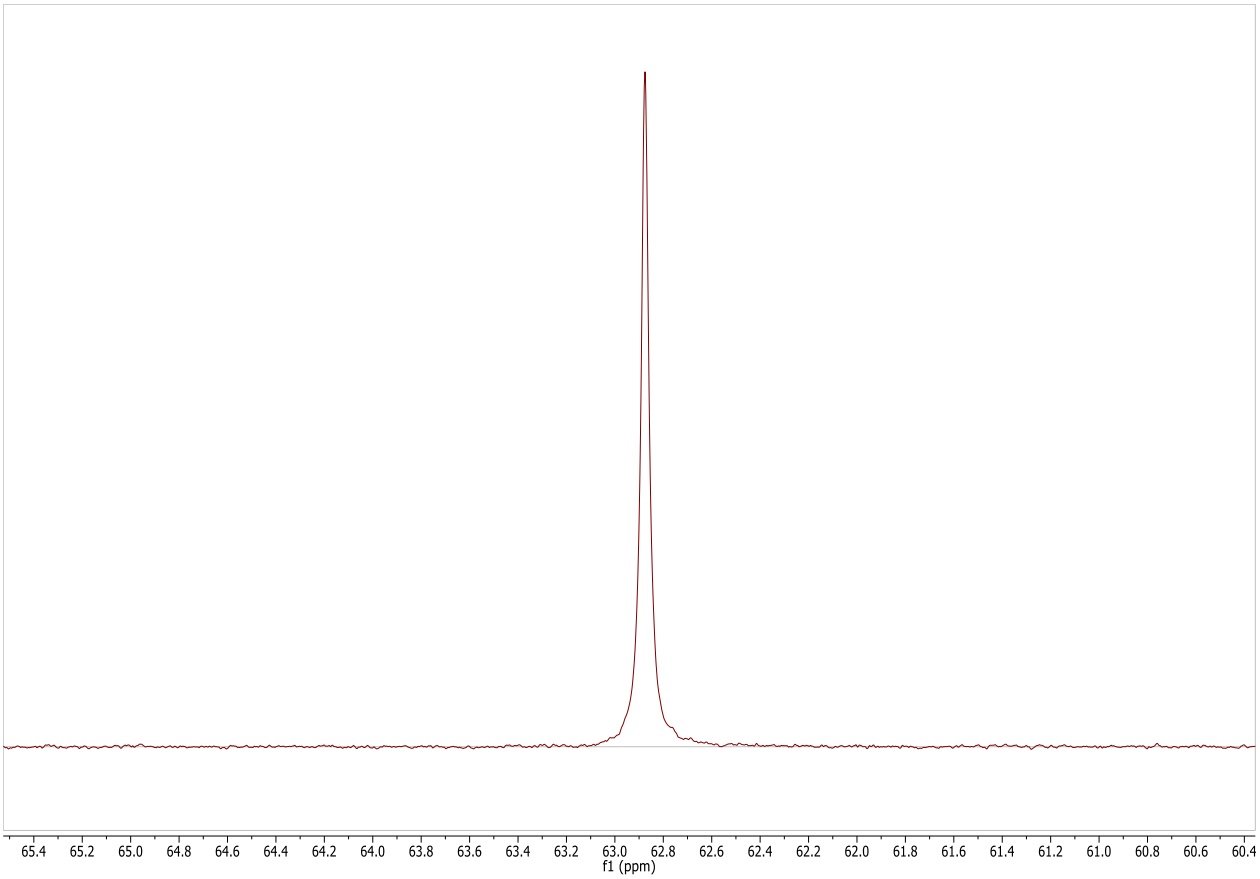

Compound 2. [Au(SC_6HF_4-4)($PC_{20}H_{27}$)].

^{1H}-NMR

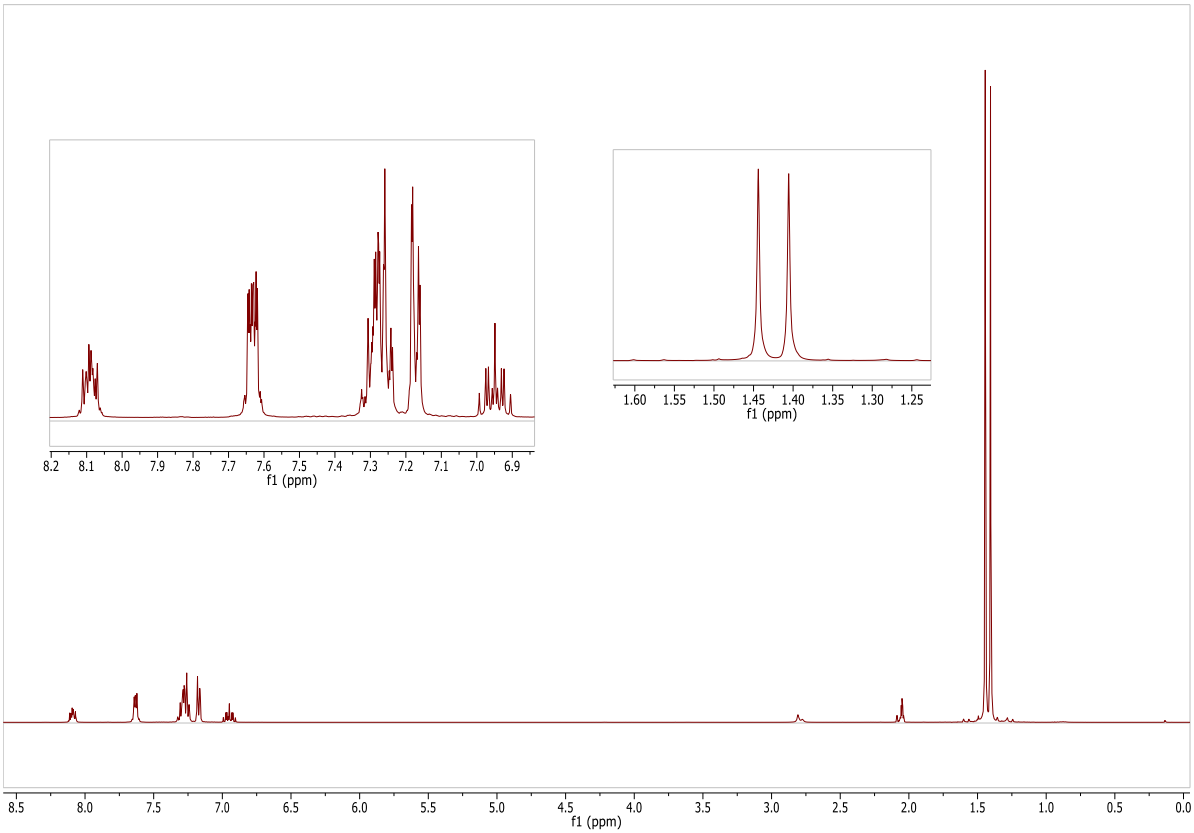

^{19}F-NMR

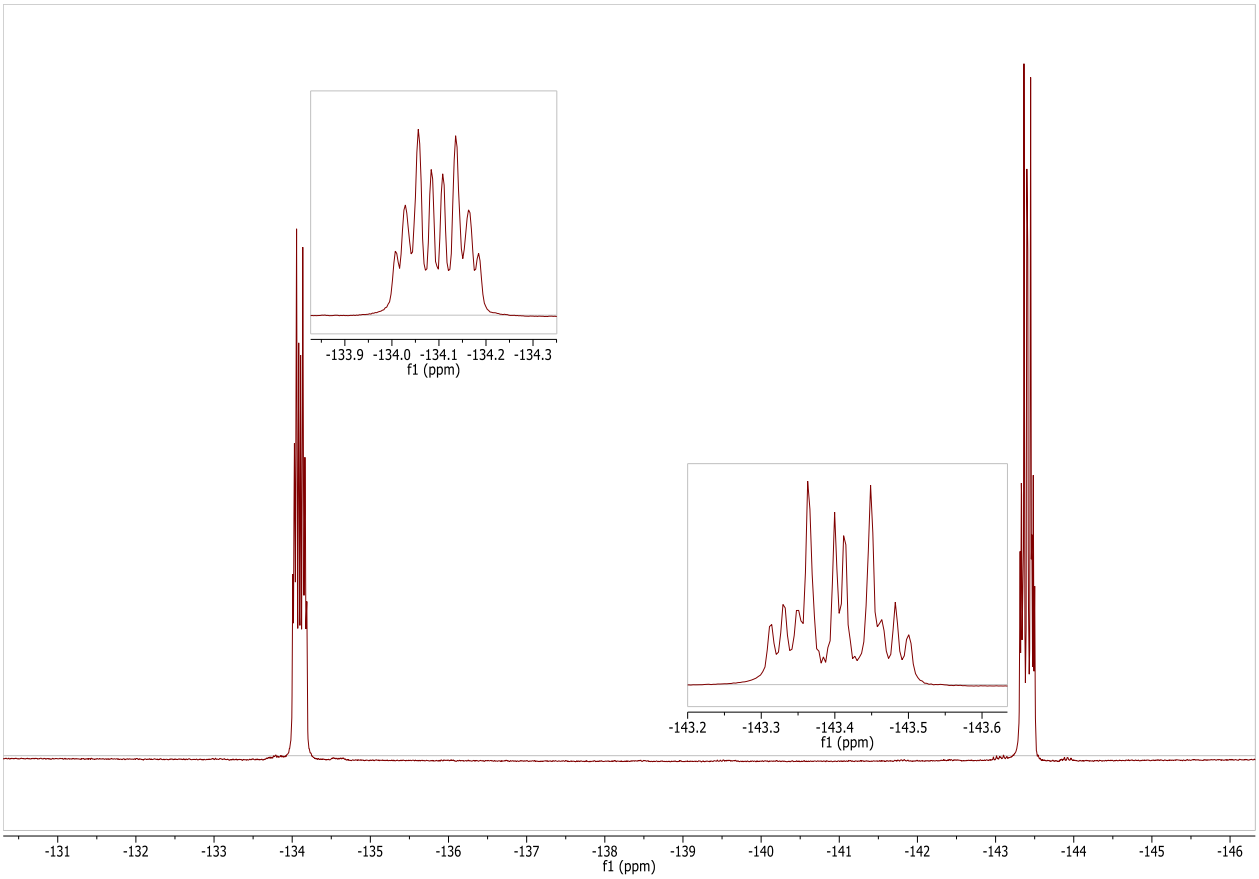

^{13}C-NMR

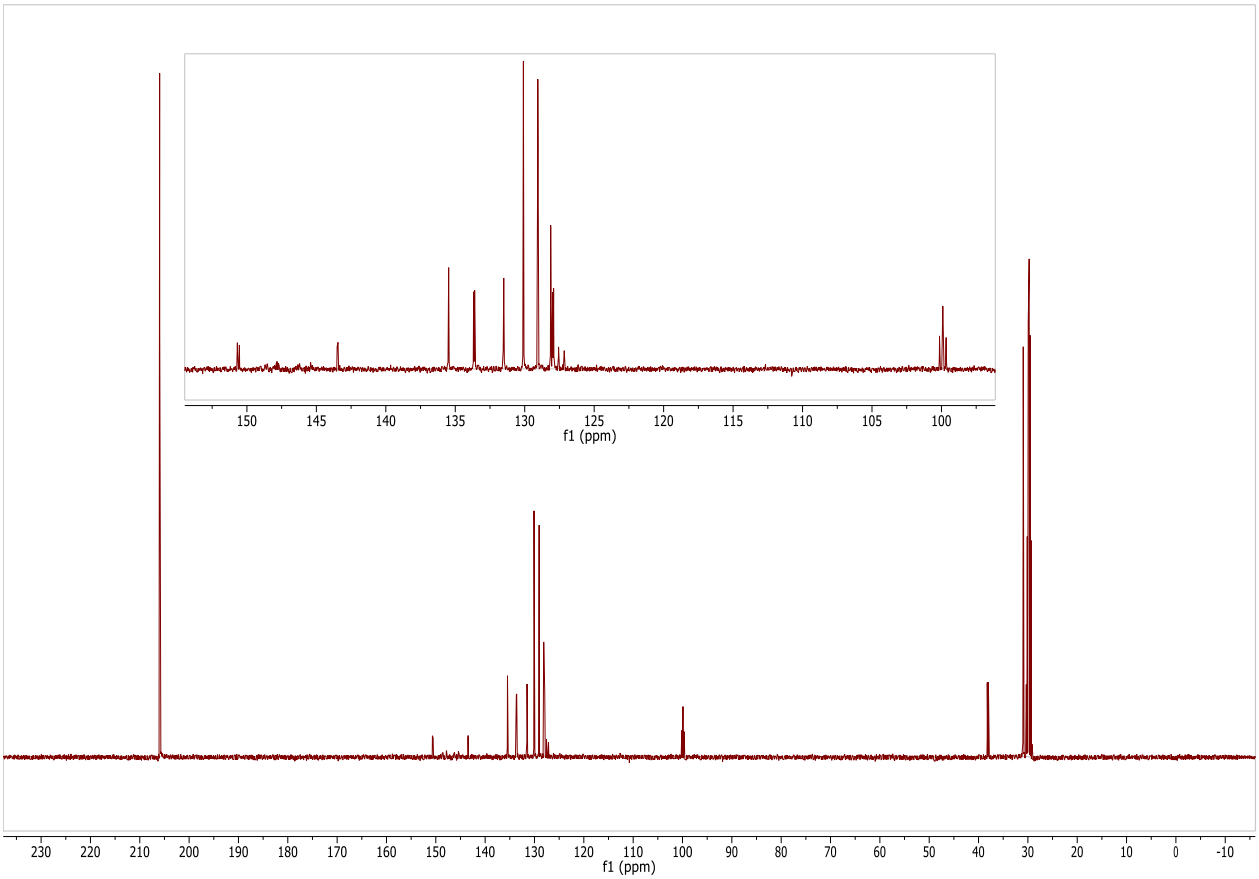

^{31}P-NMR

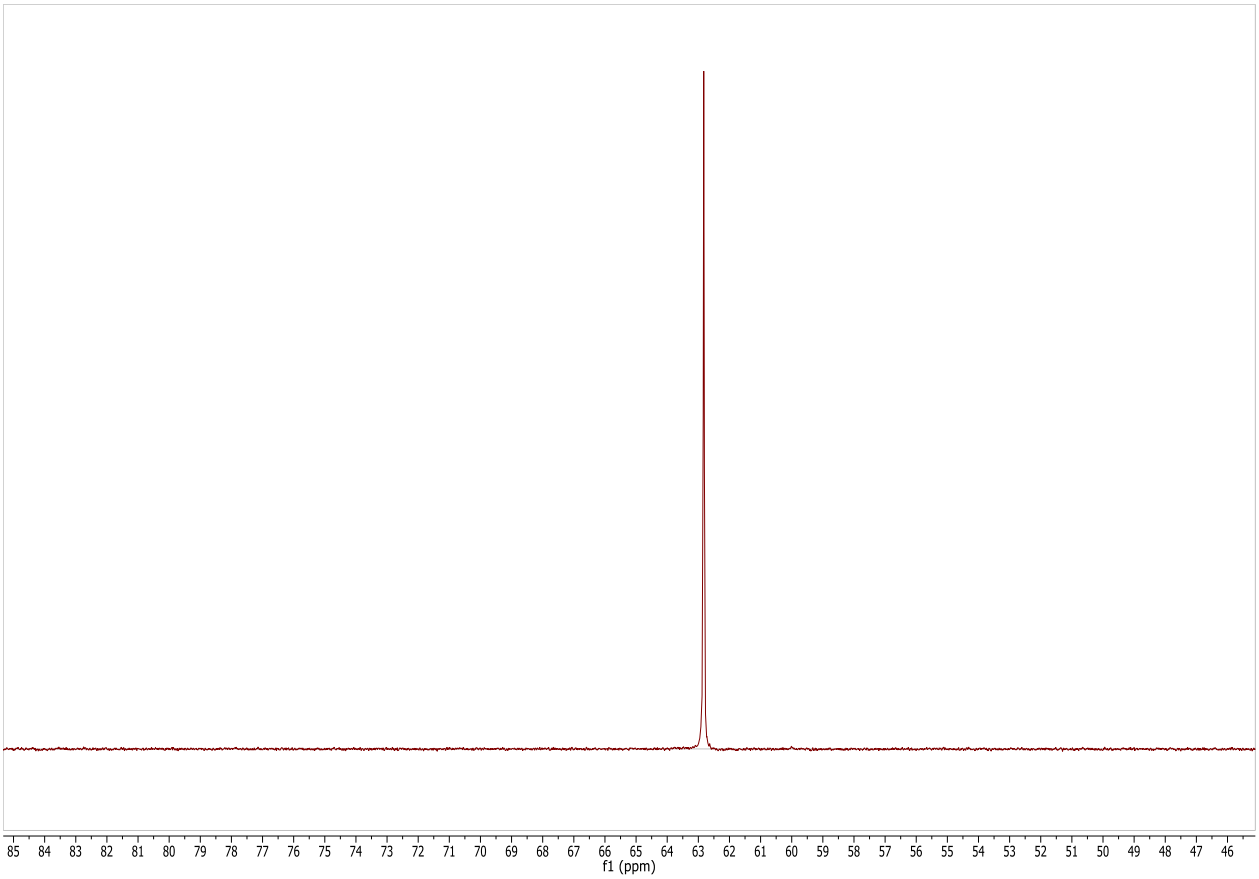

Compound 3. [Au($SC_6H_3F_2$-3,5)($PC_{20}H_{27}$)].

^{1}H-NMR

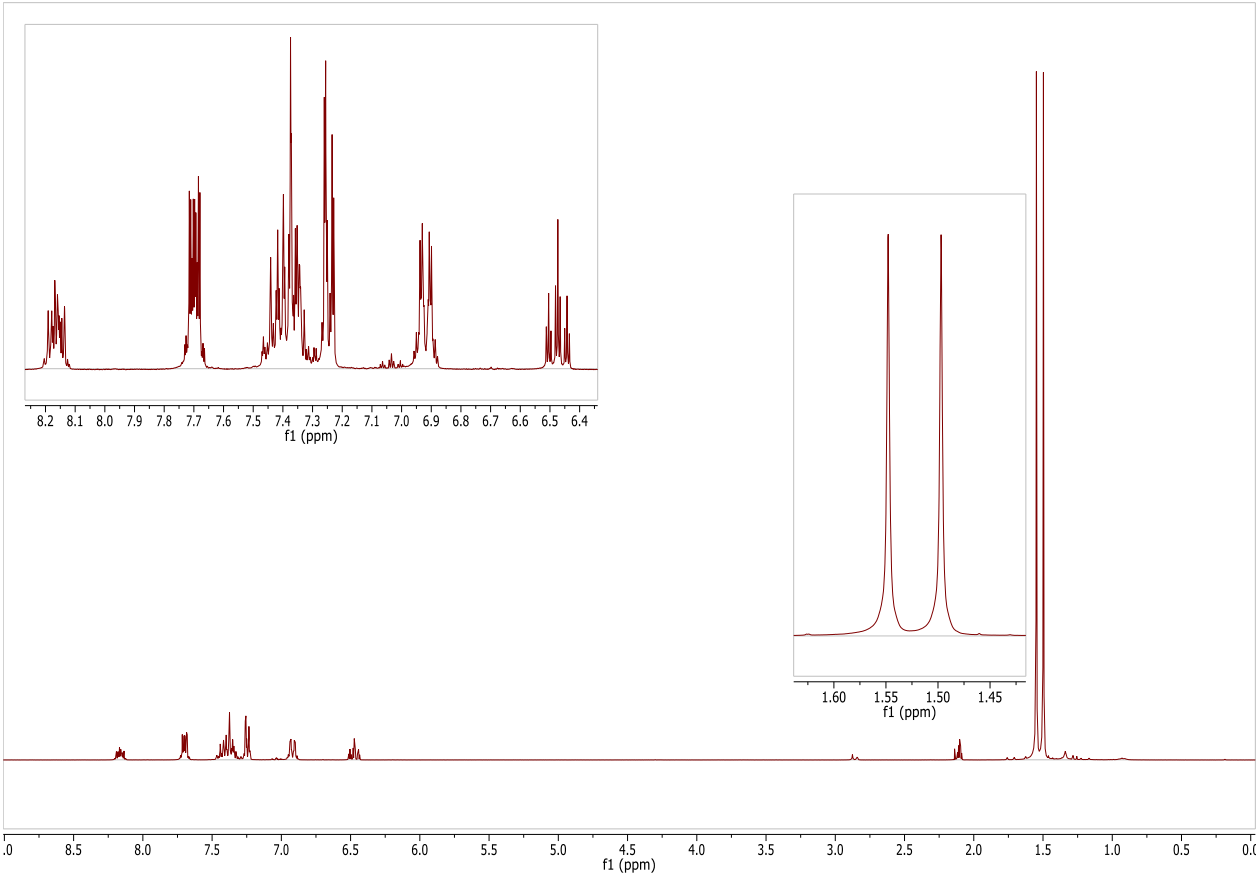

^{19}F-NMR

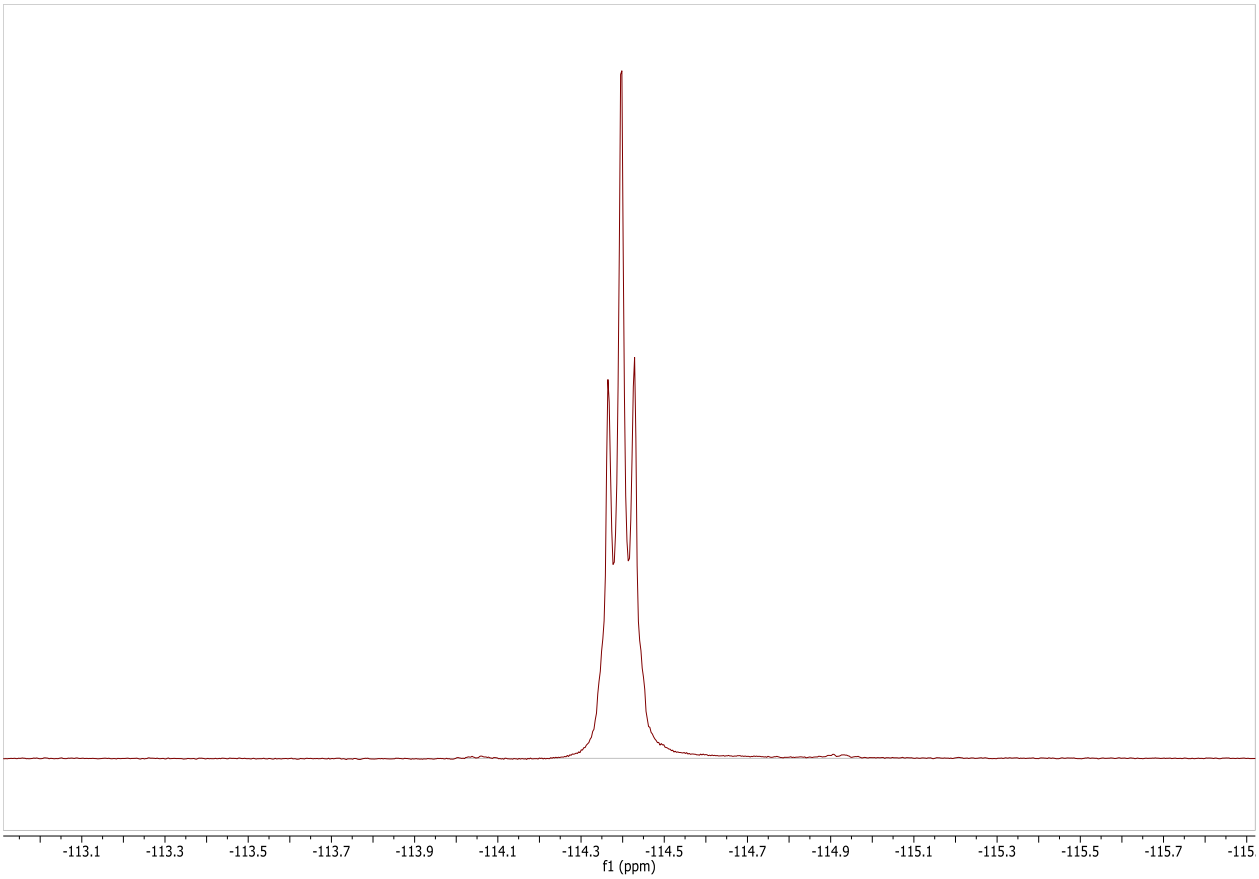

^{13}C-NMR

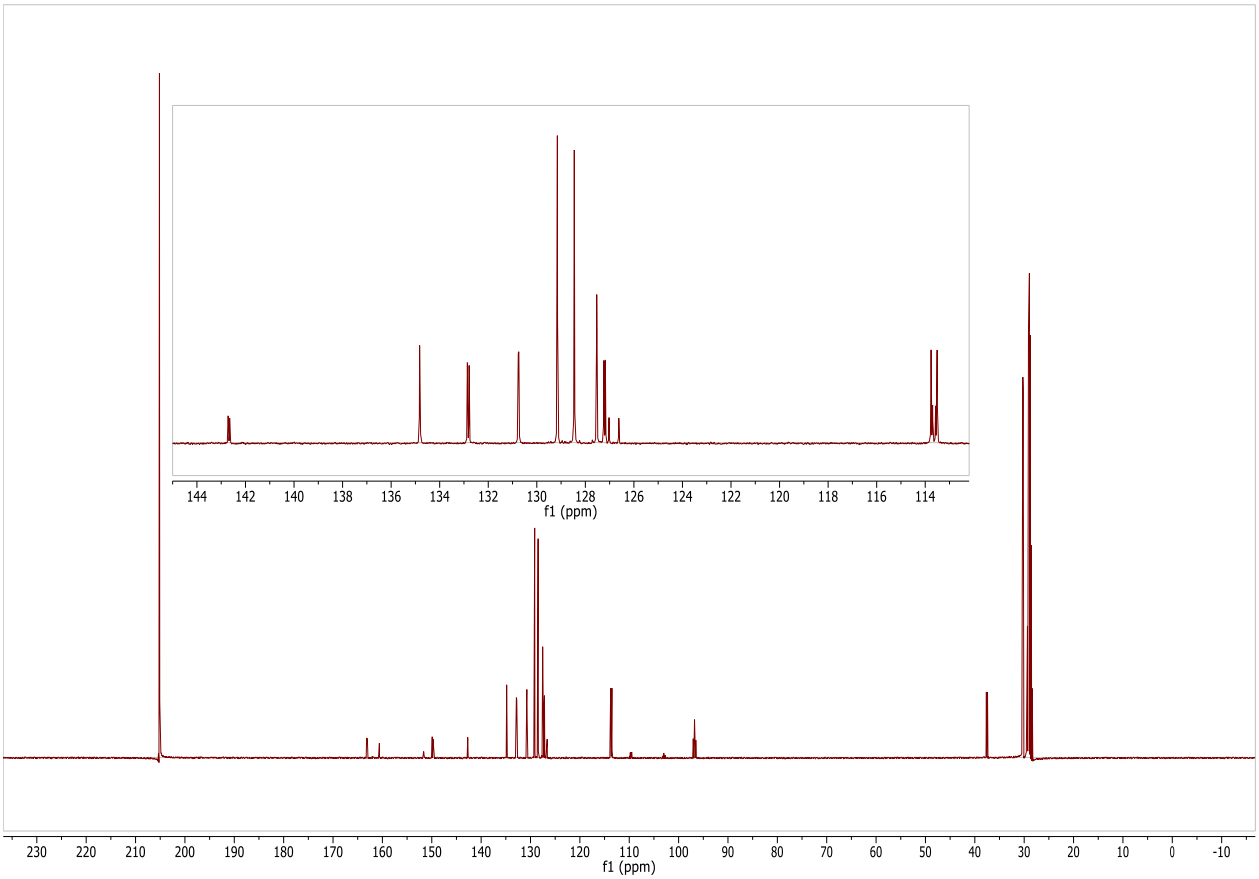

^{31}P-NMR

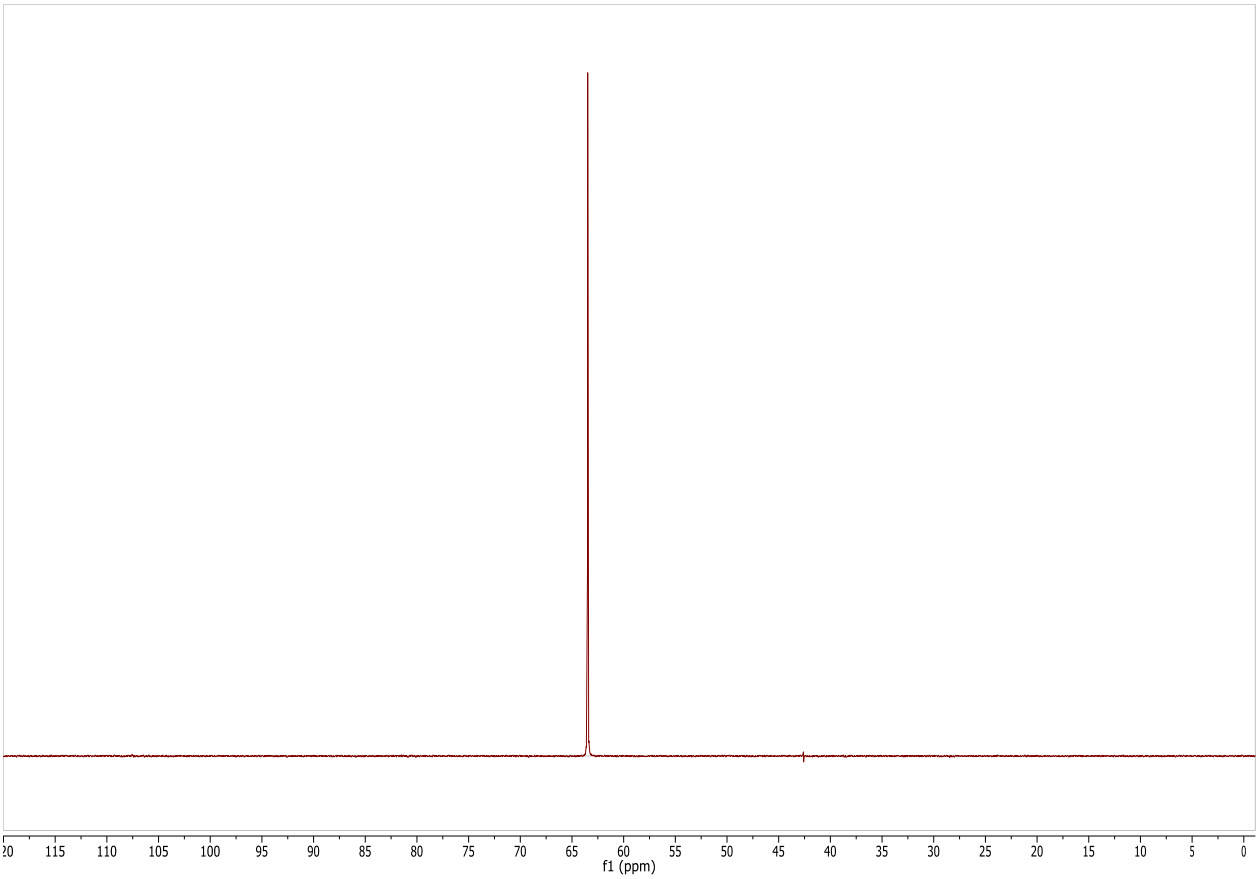

Compound 4. [Au($SC_6H_3F_2$-2,4)($PC_{20}H_{27}$)]

^{1}H-NMR

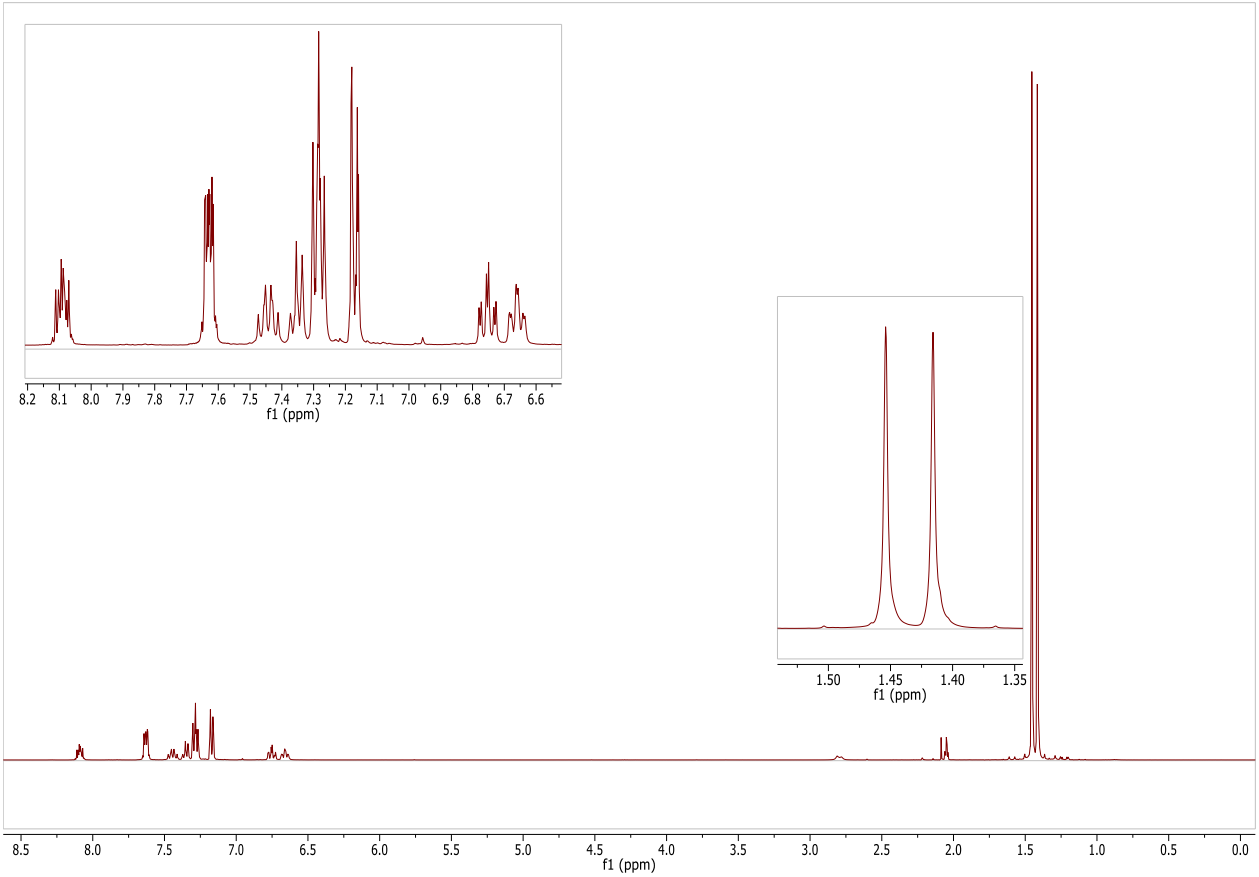

^{19}F-NMR

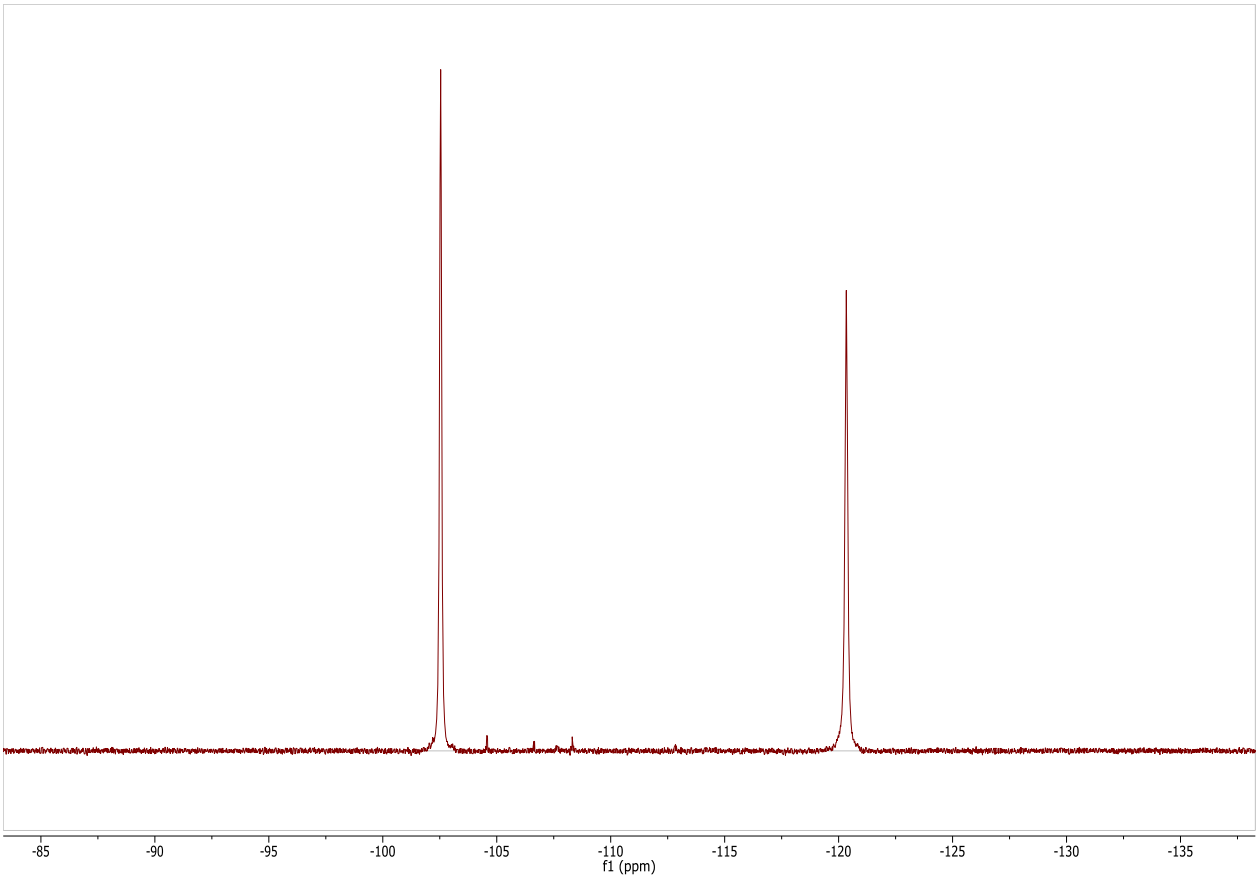

^{13}C-NMR

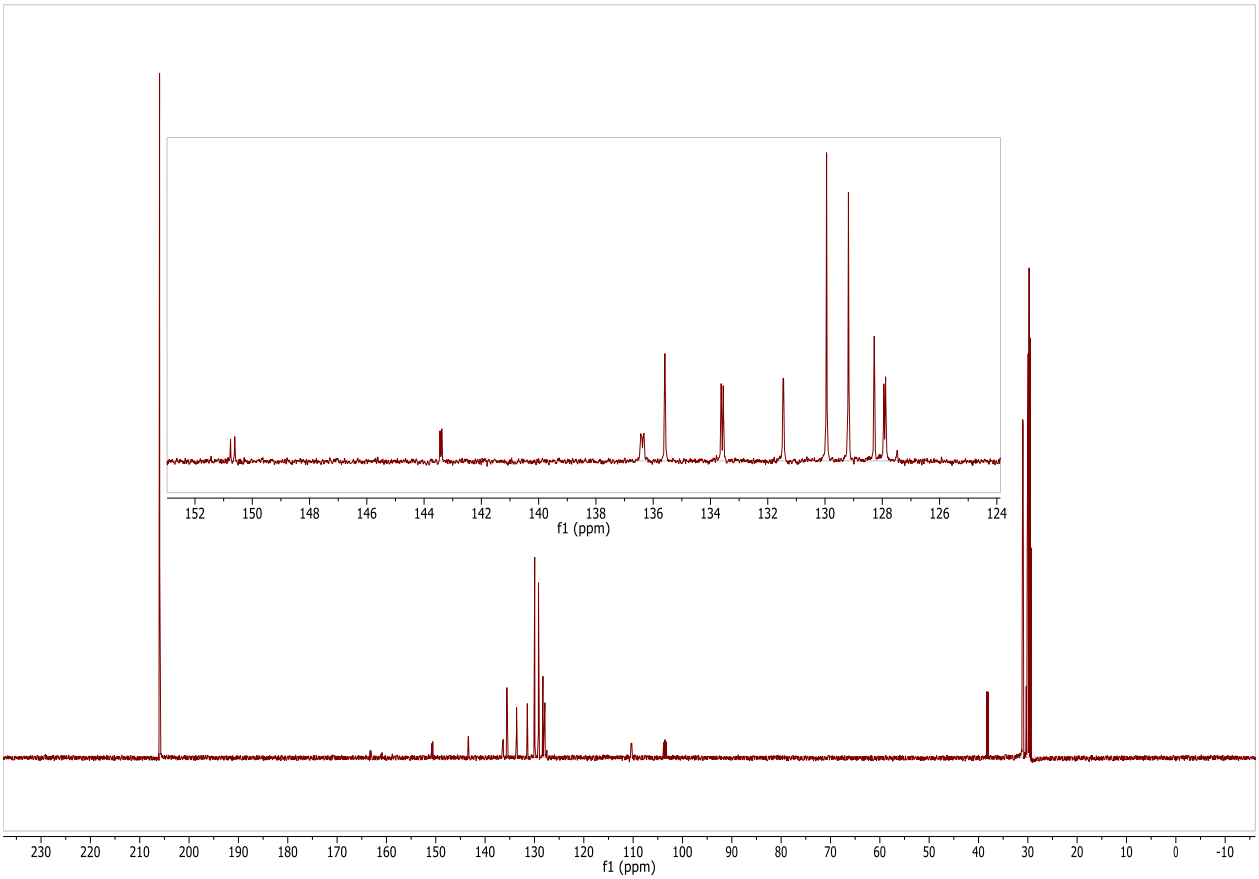

^{31}P-NMR

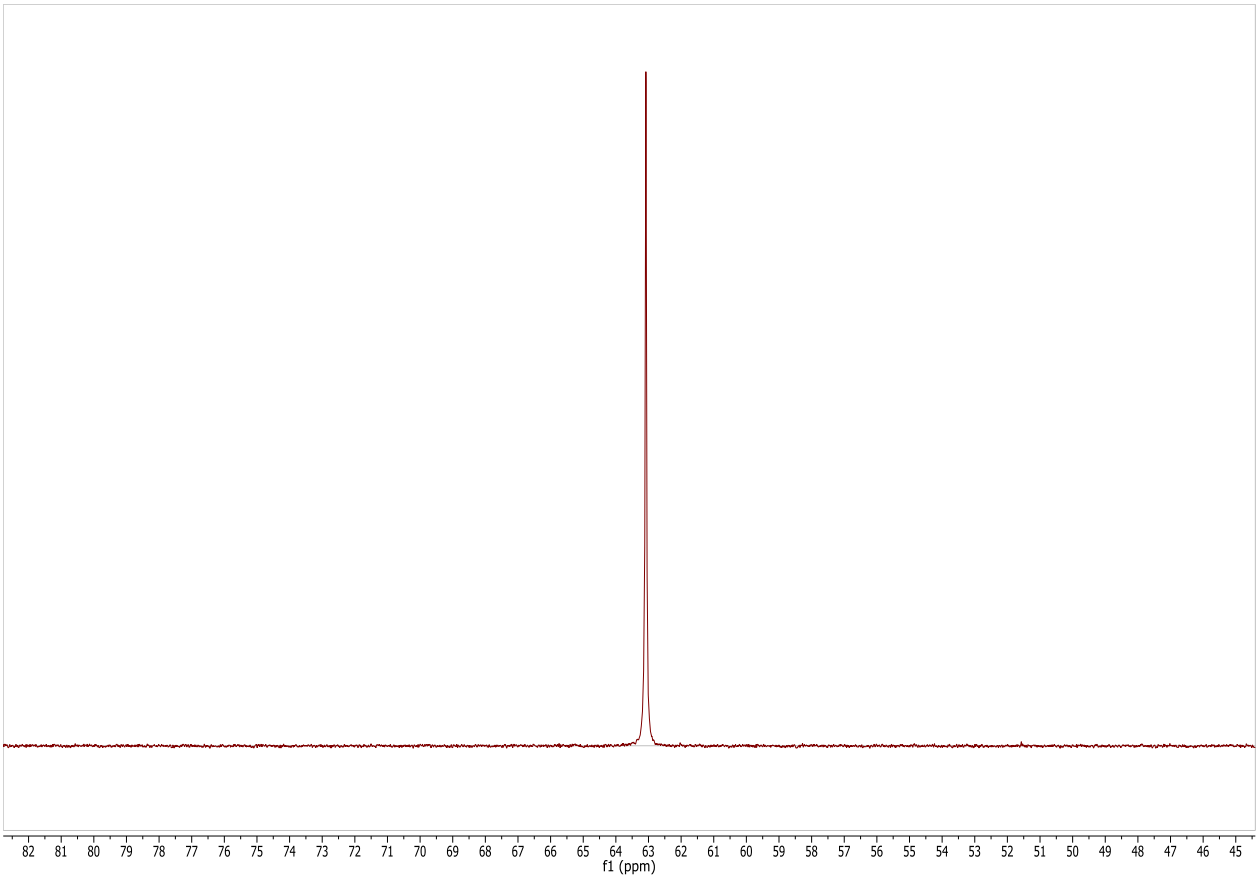

Compound 5. [Au(SC_6H_4F-2)($PC_{20}H_{27}$)].

^{1}H-NMR

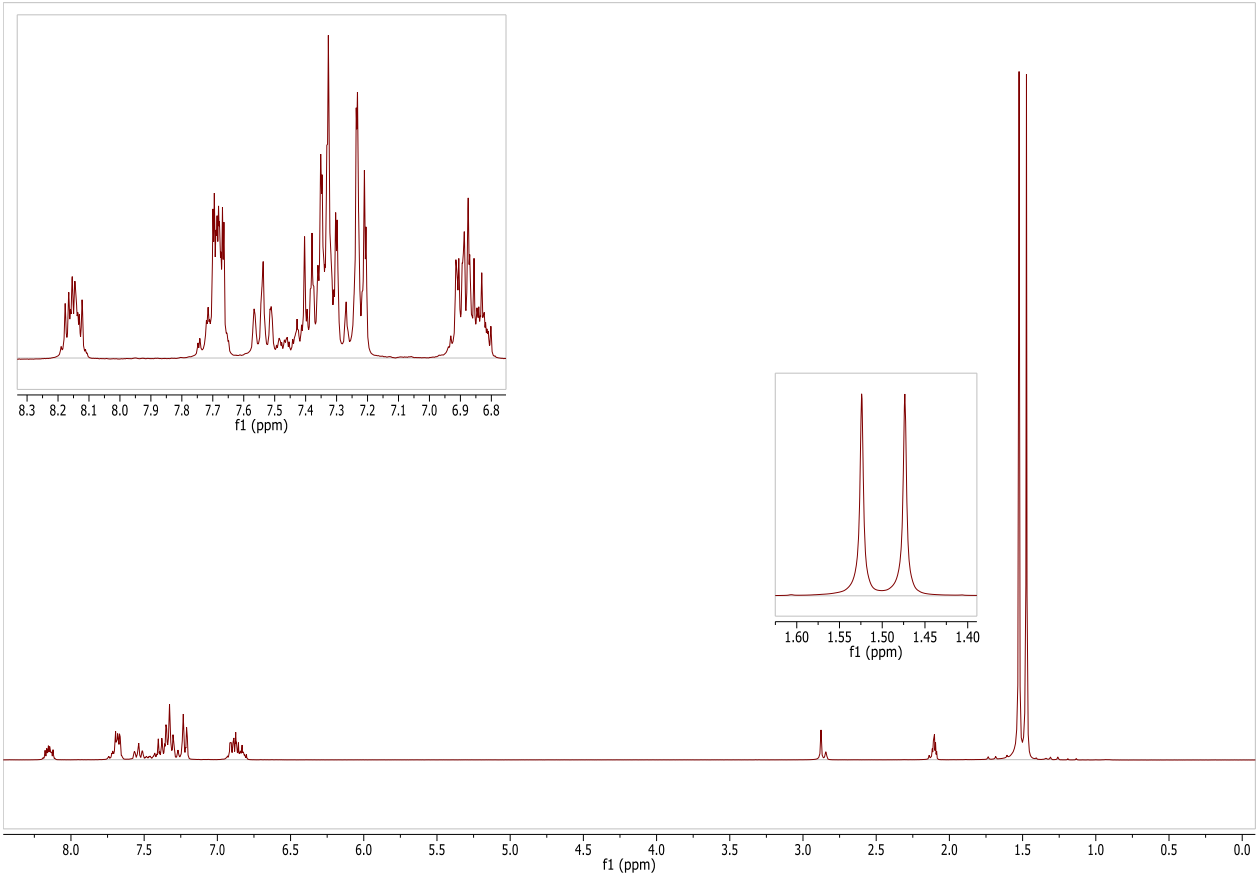

^{19}F-NMR

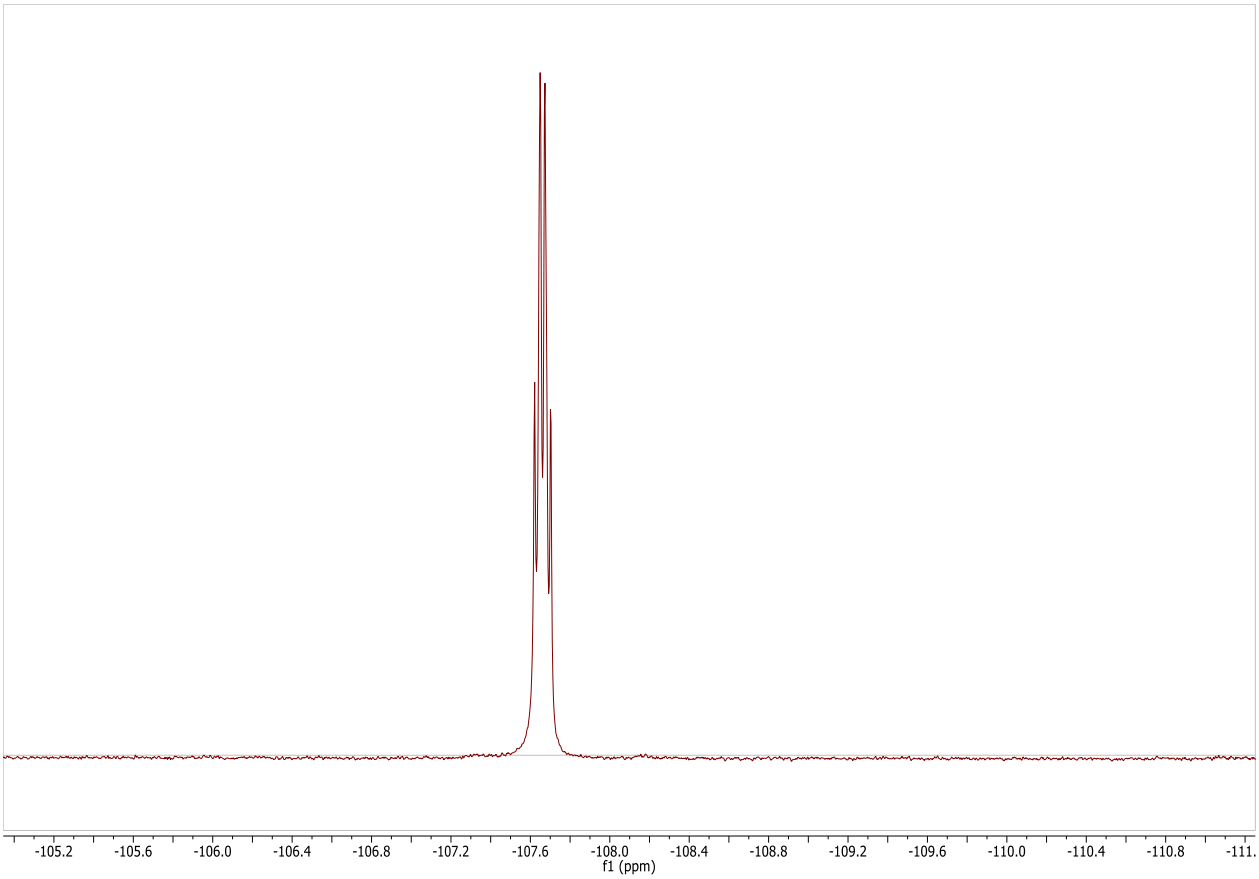

^{13}C-NMR

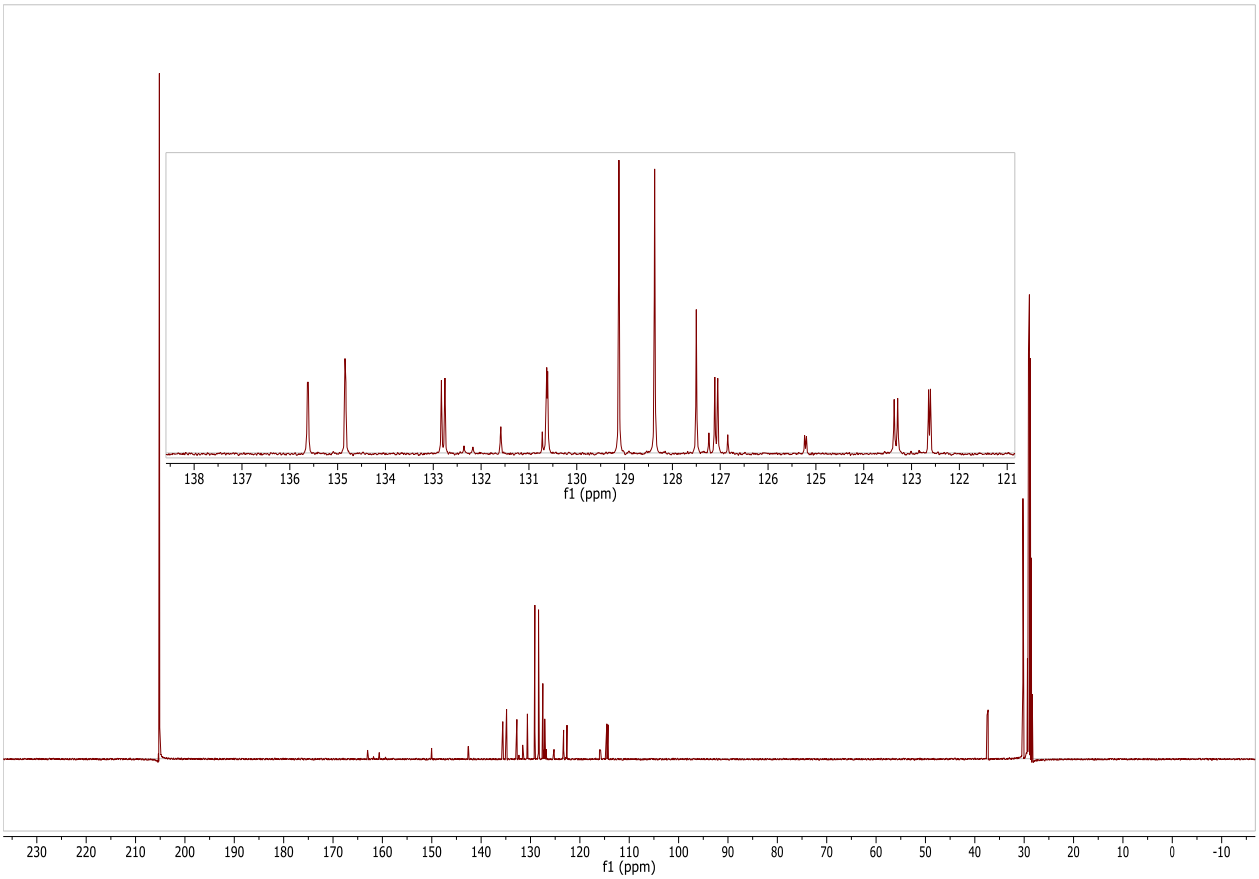

^{31}P-NMR

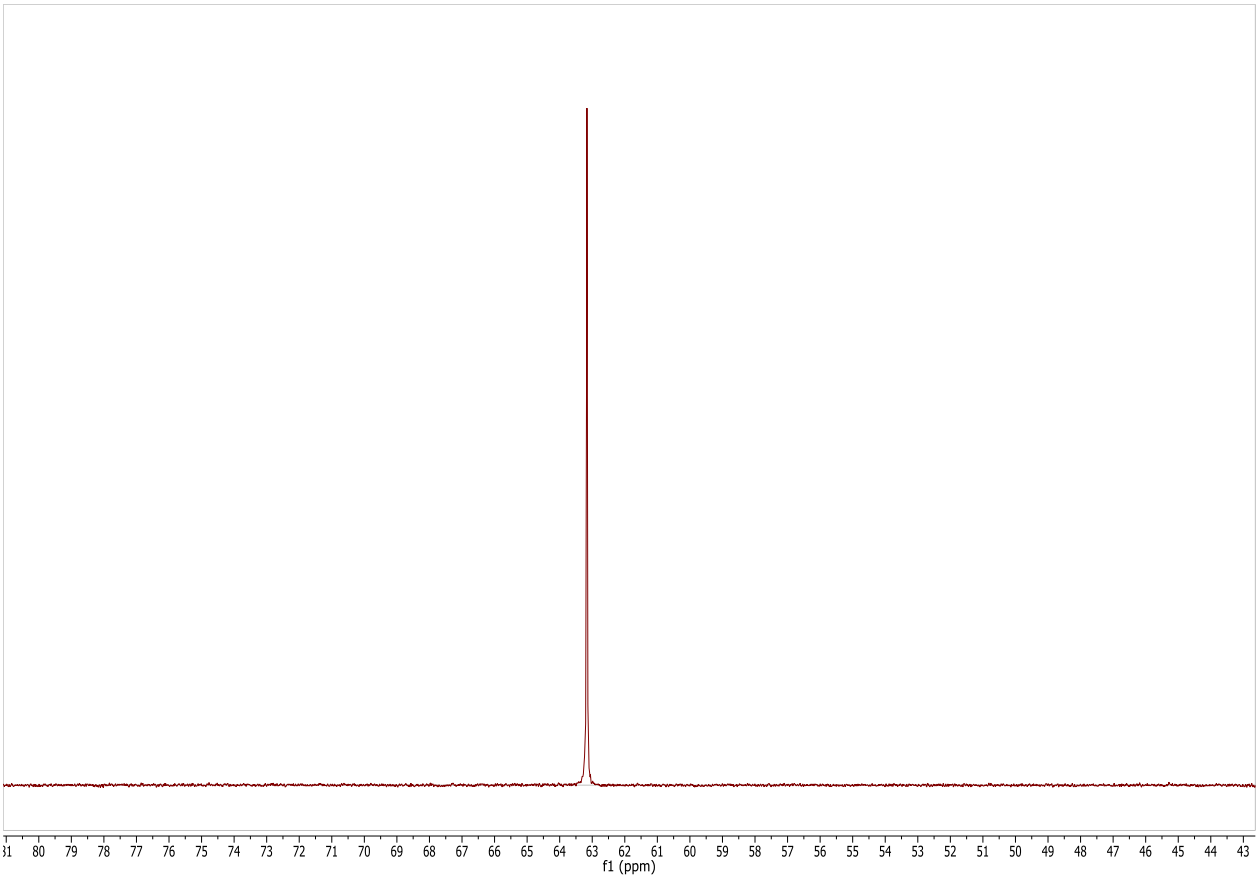

Compound 6. [Au(SC_6H_4F-3)($PC_{20}H_{27}$)].

^{1}H-NMR

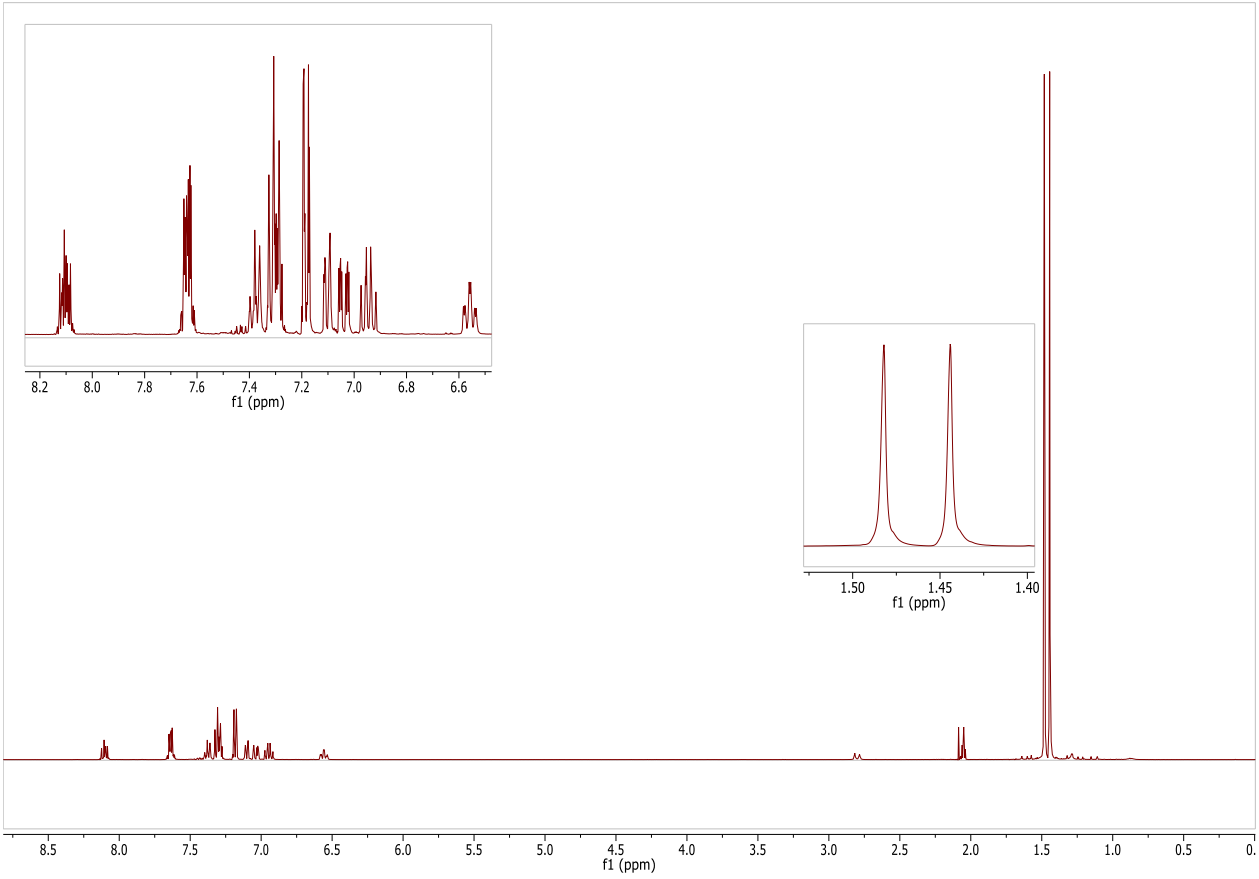

^{19}F-NMR

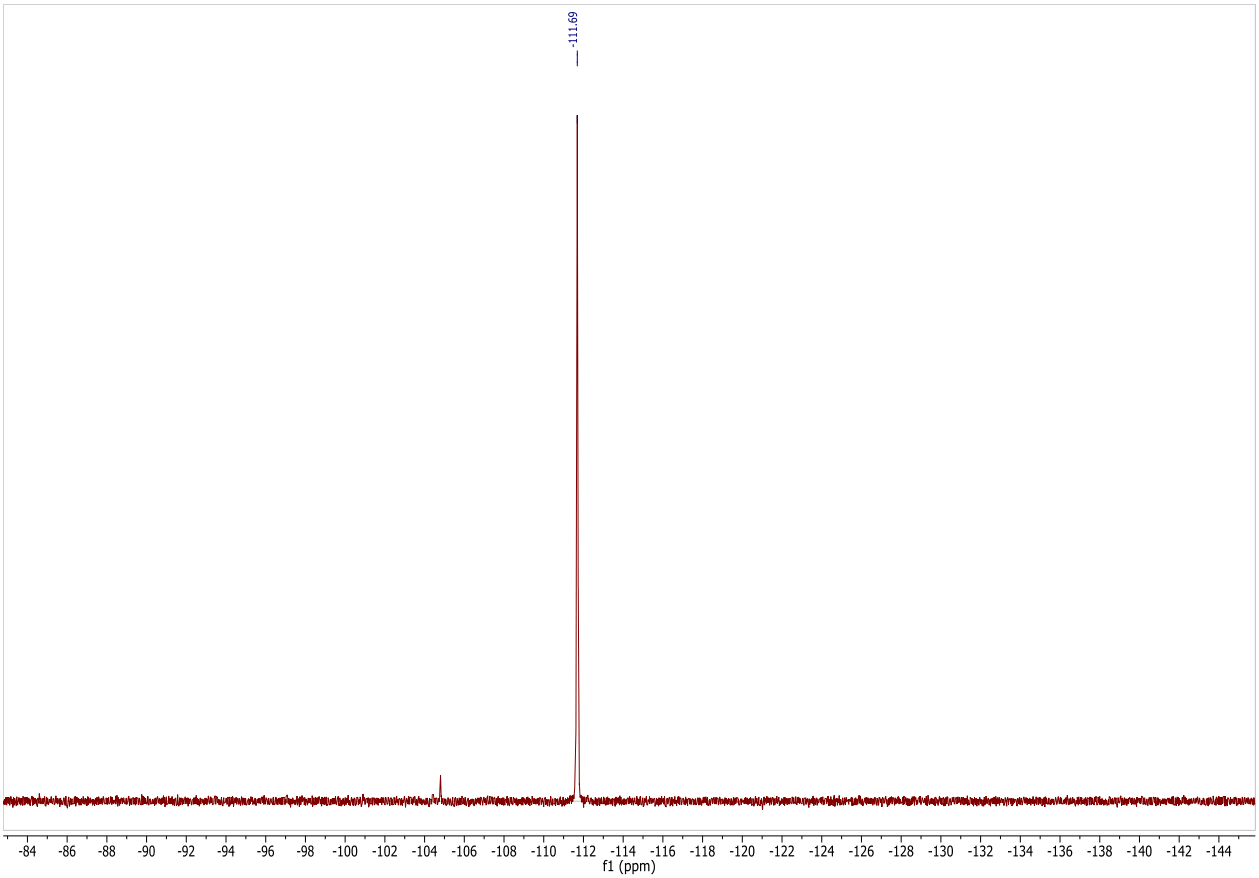

Note 2: ^{19}F NMR spectra of compound 5 shows a residual secondary signal probably because of a slow decomposition of the product in solution.

^{13}C-NMR

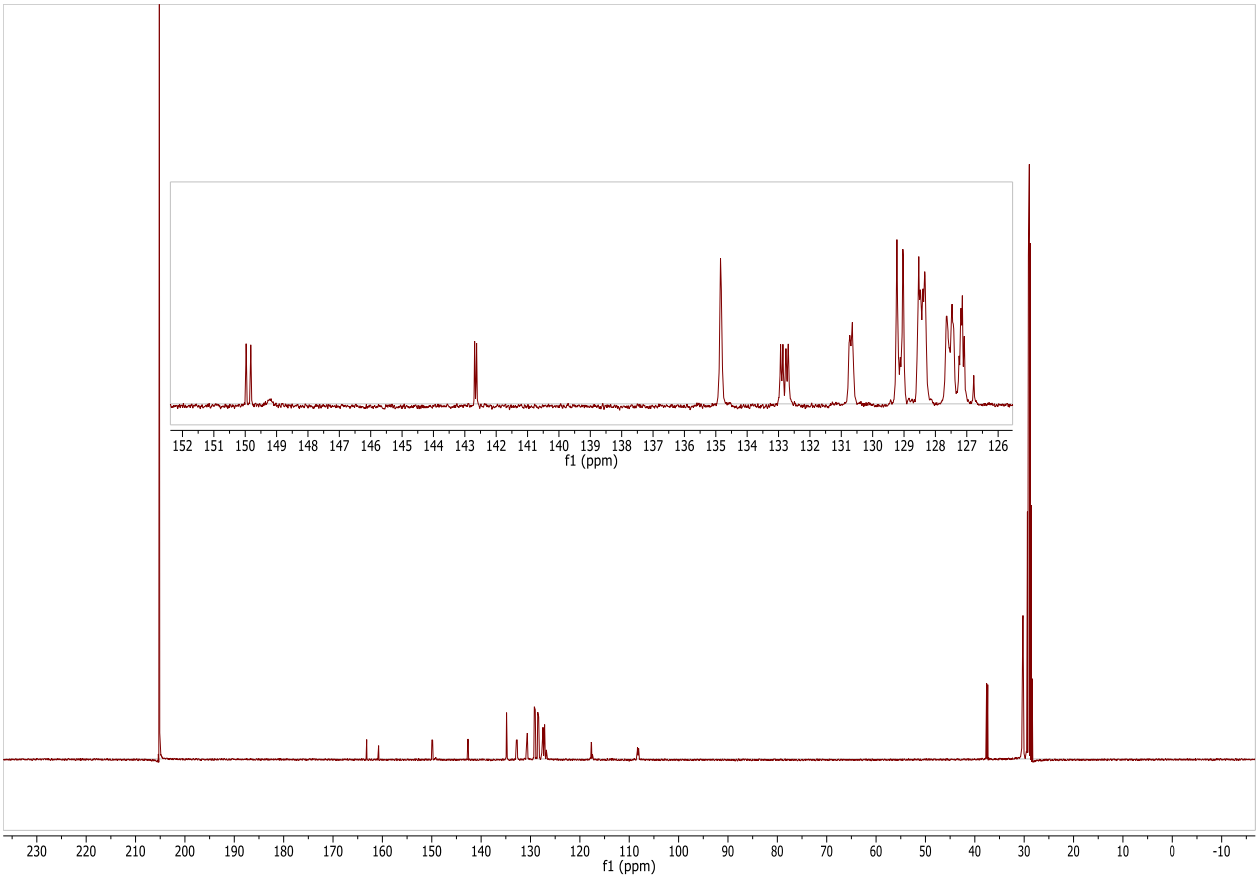

^{31}P-NMR

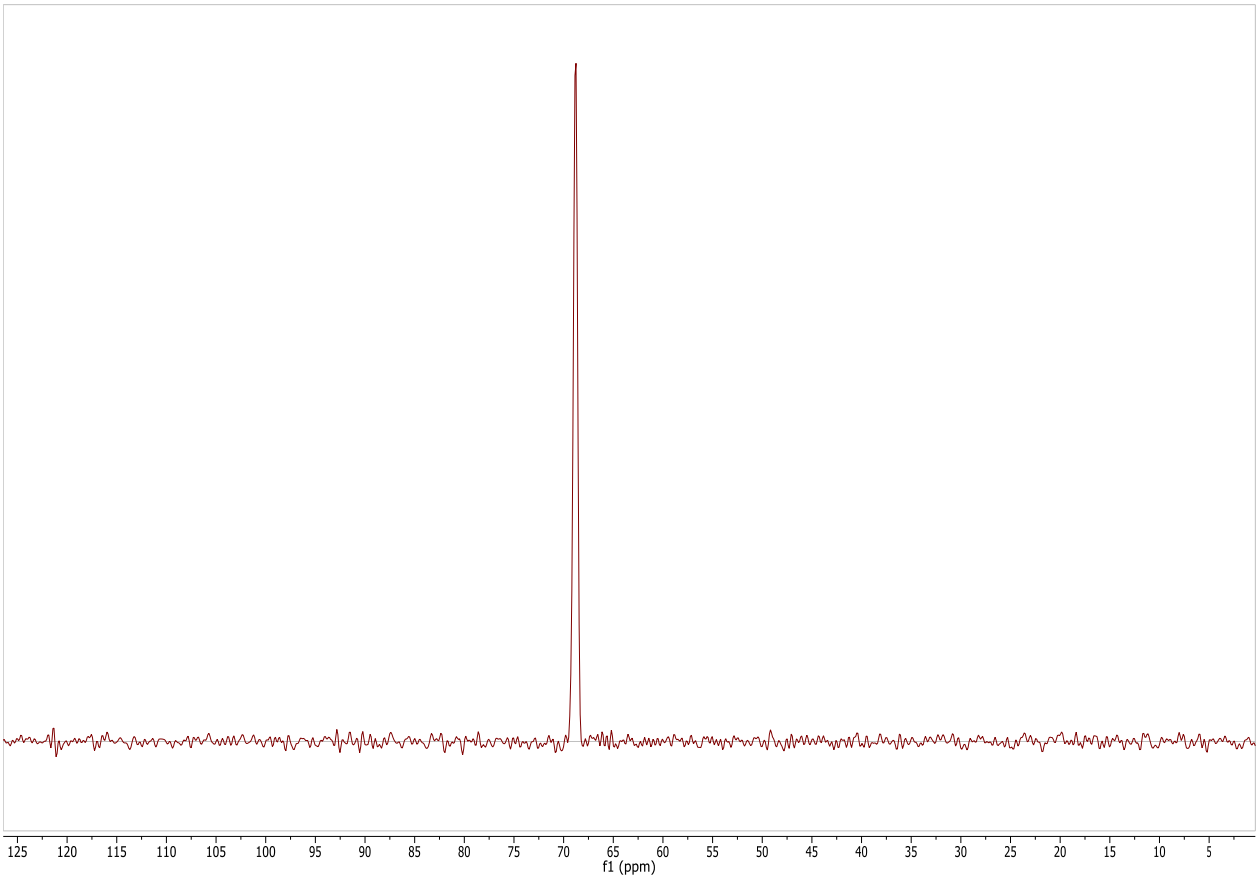

Compound 7. [Au(SC_6H_4F-4)($PC_{20}H_{27}$)].

^{1}H-NMR

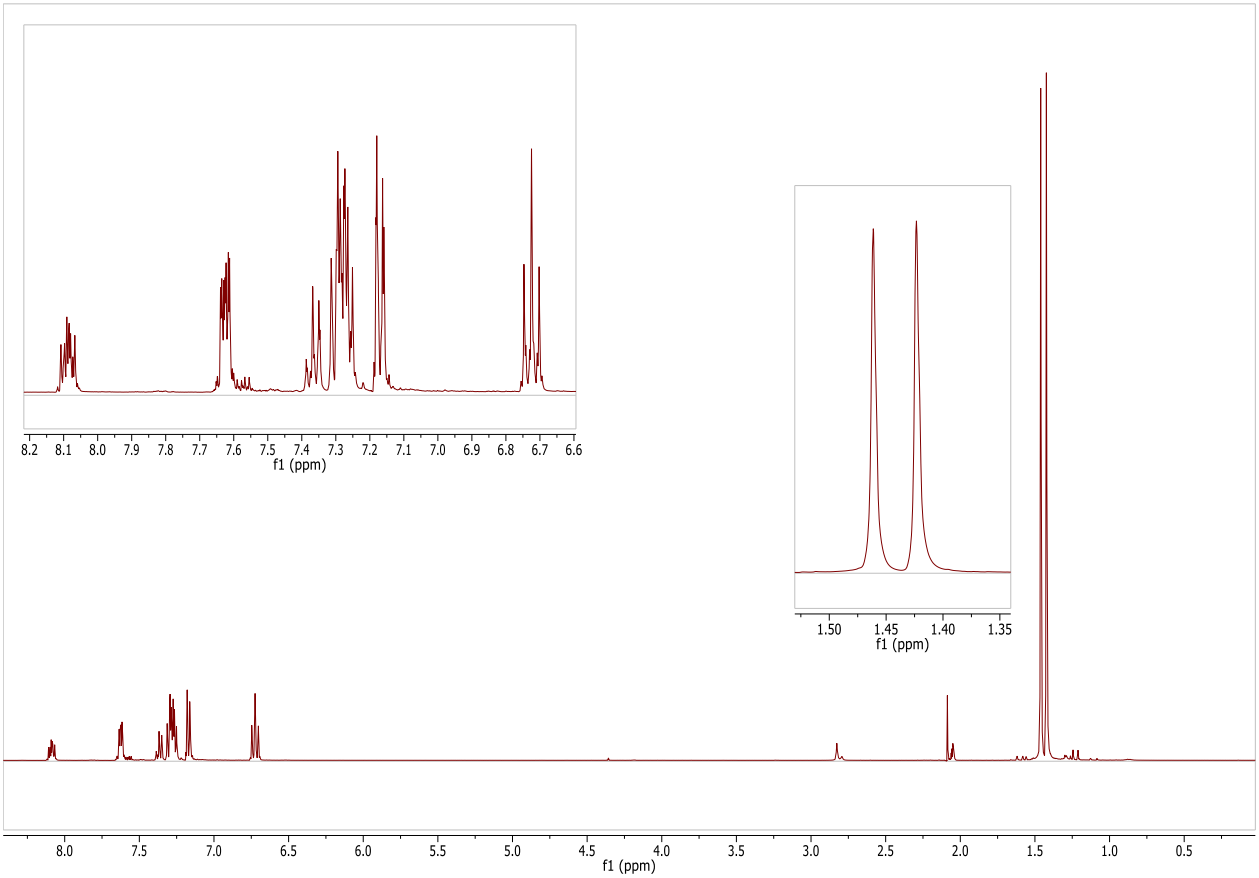

^{19}F-NMR

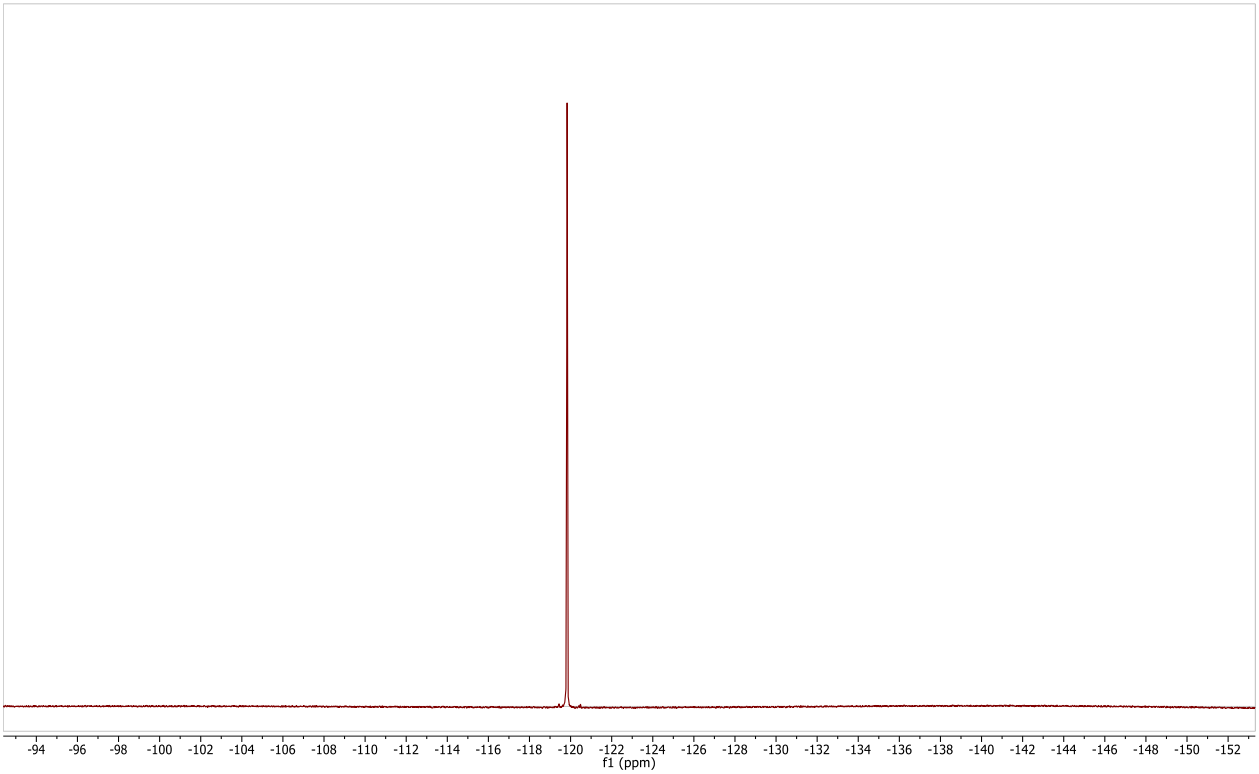

^{13}C-NMR

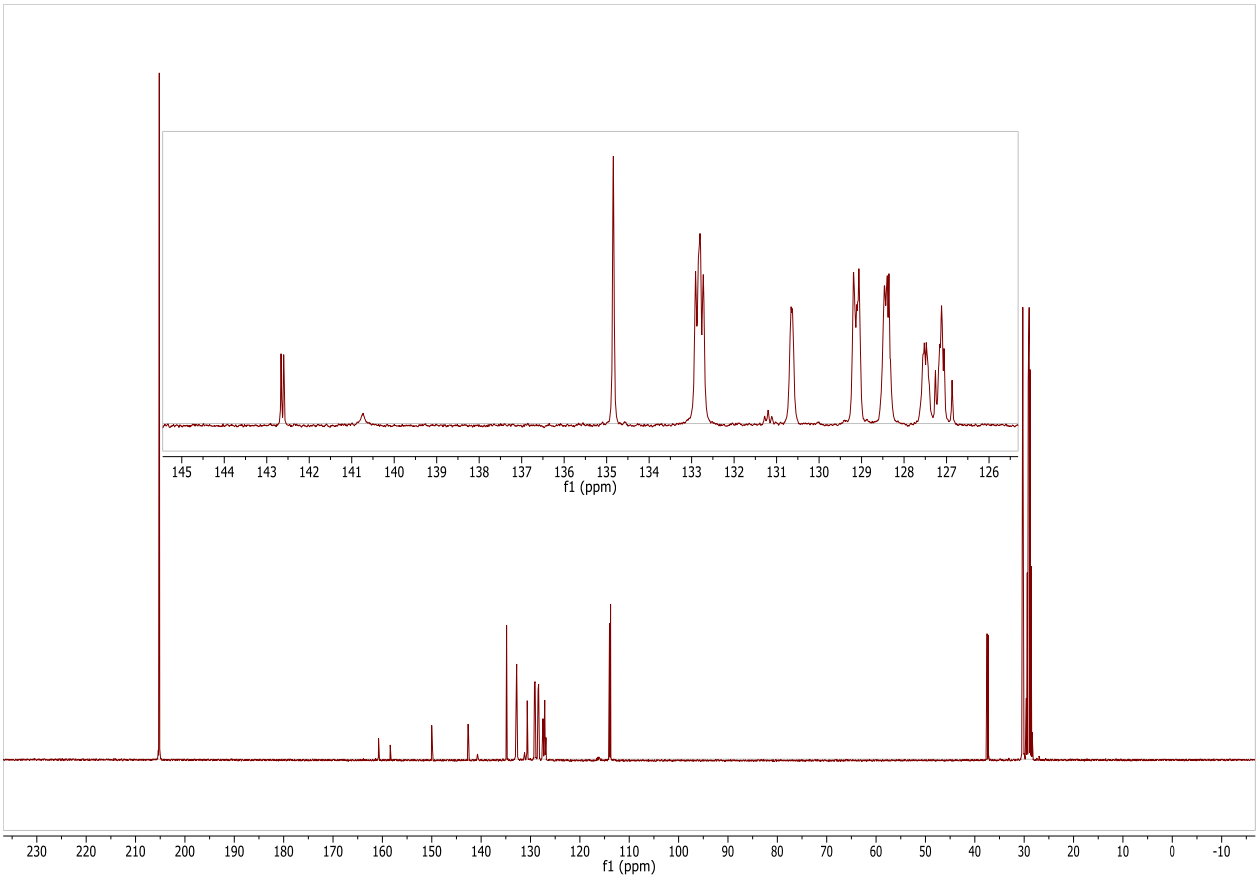

^{31}P-NMR

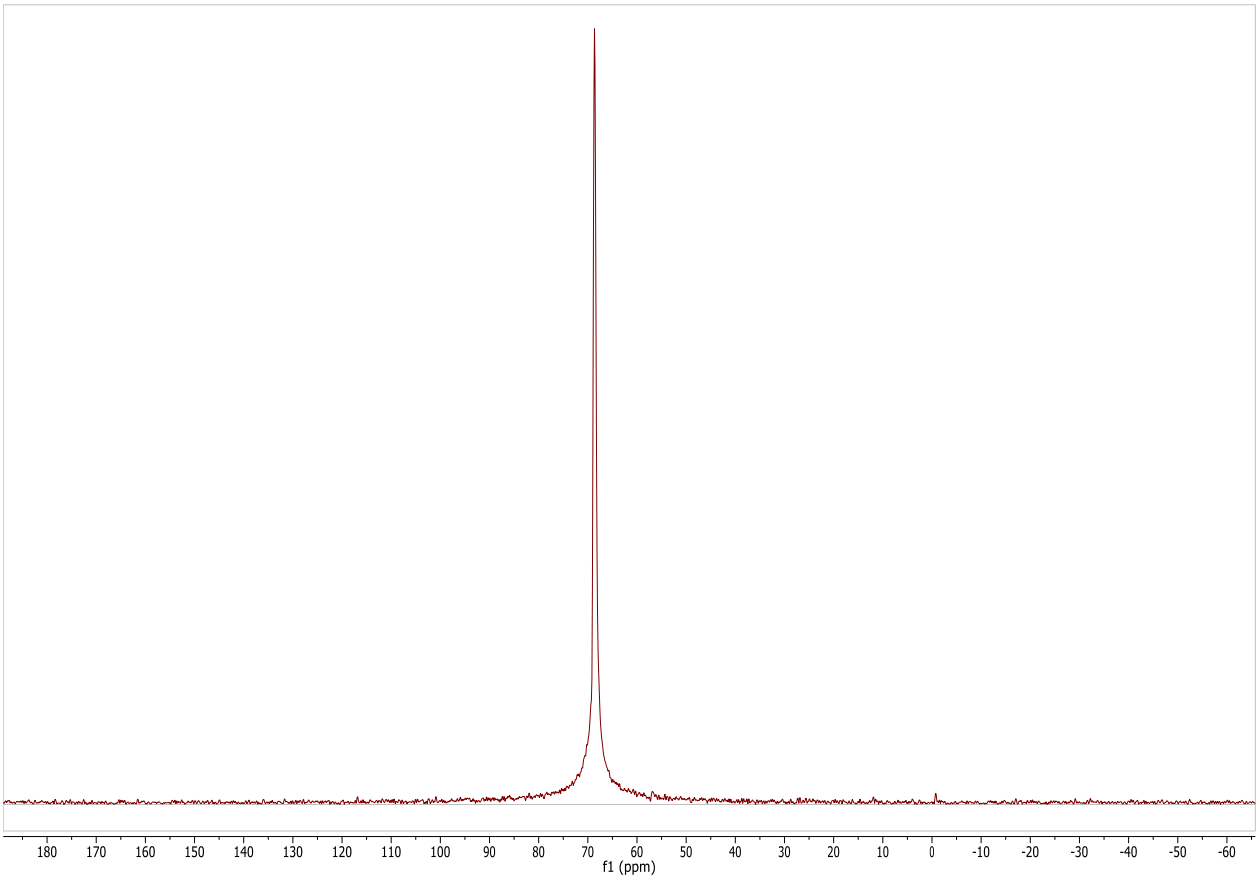

Compound 8. [$Au(SCF_3)(PC_{20}H_{27})$].

^{1}H-NMR

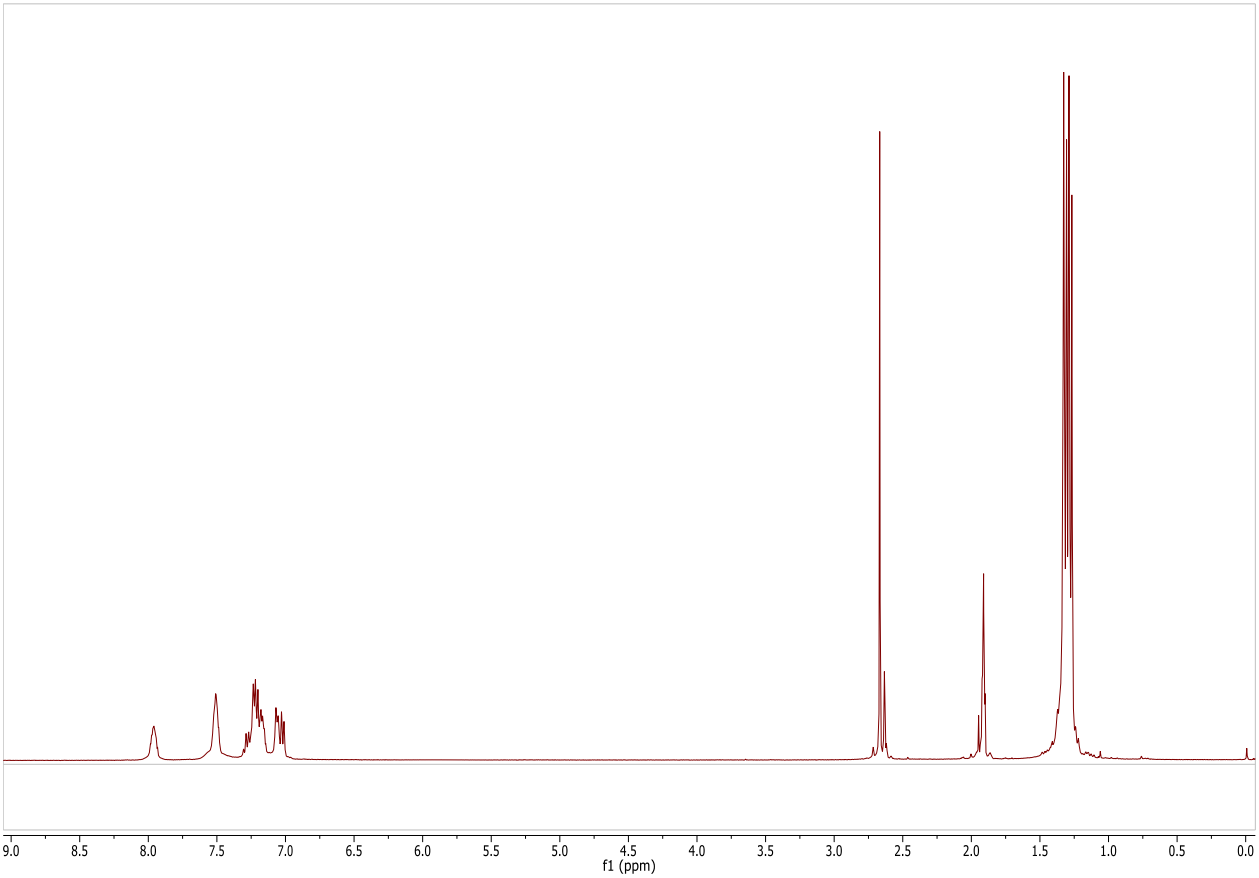

^{19}F-NMR

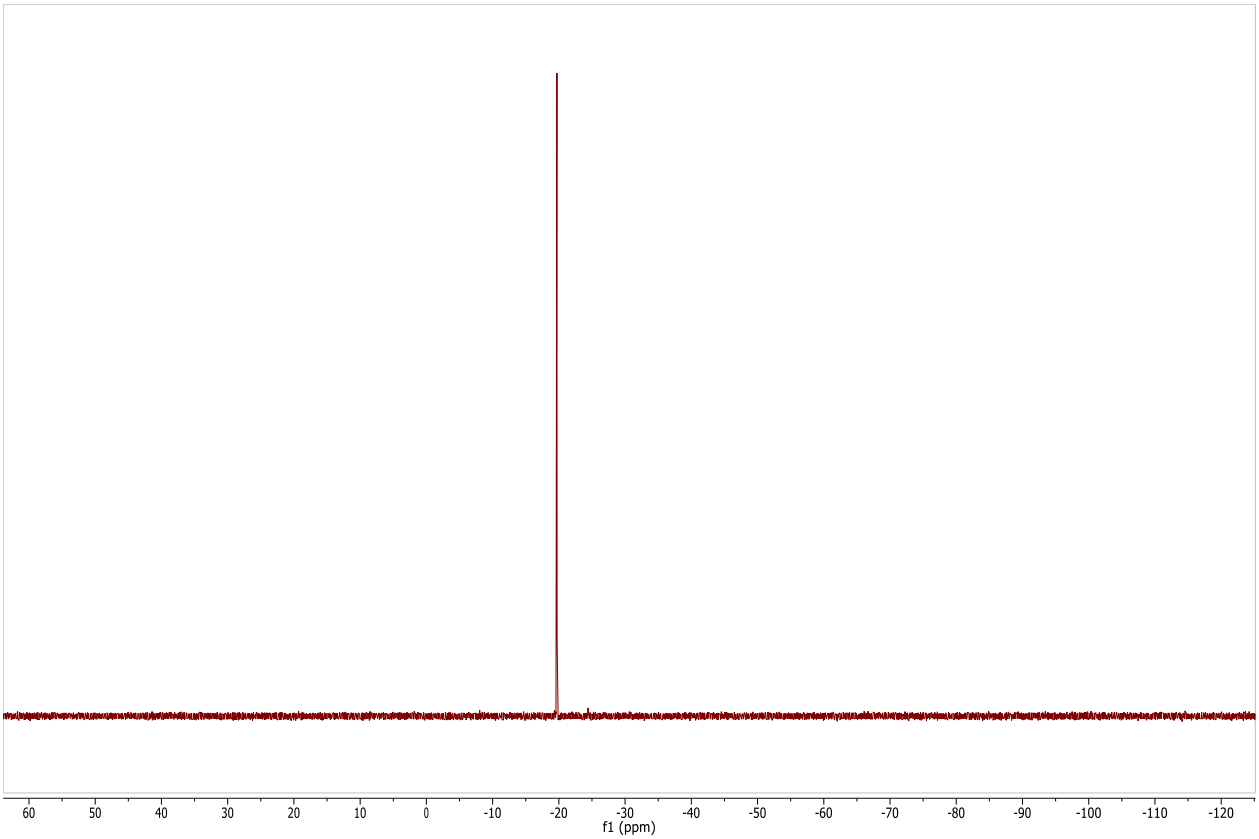

^{13}C-NMR

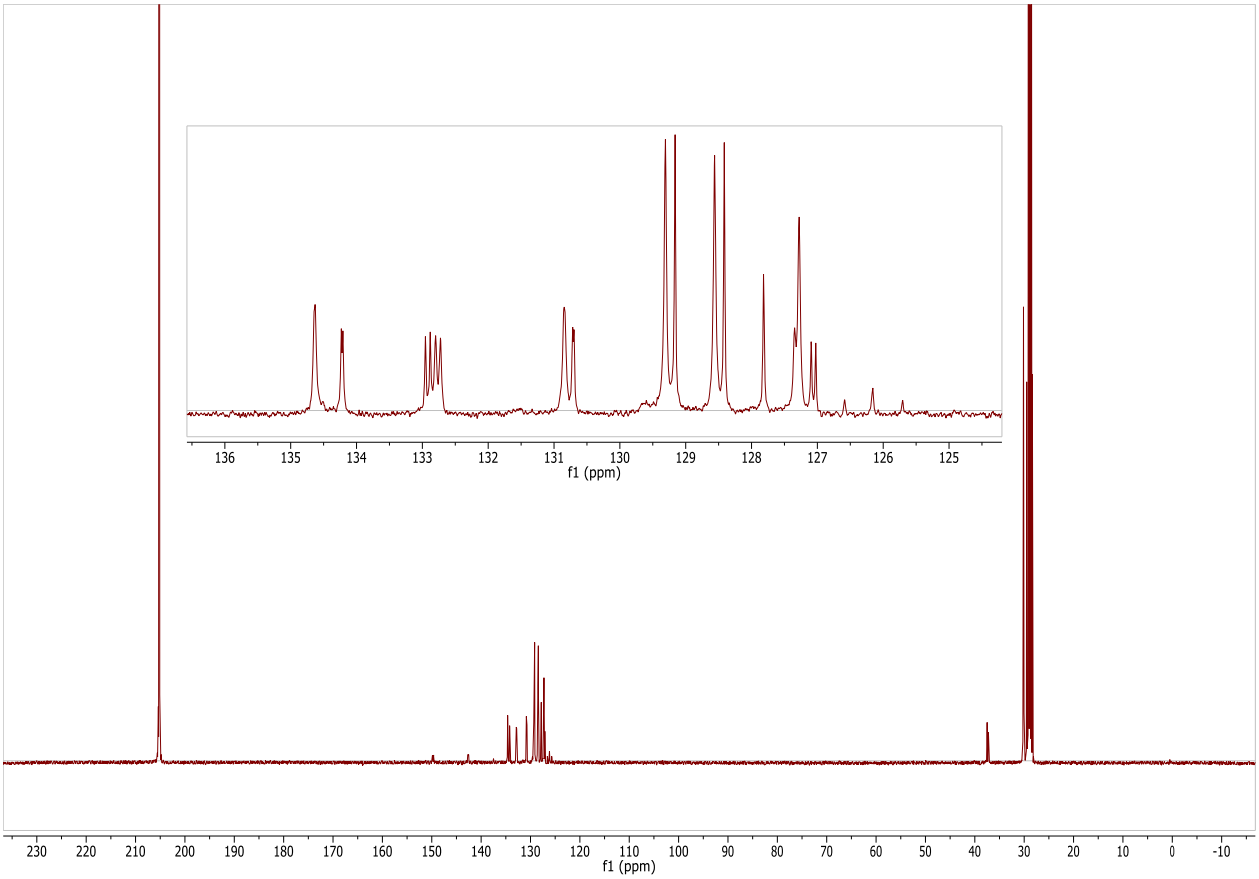
136 135 134 133 132 131 130 129 128 127 126 125
f1 (ppm)
230 220 210 200 190 180 170 160 150 140 130 120 110 100 90 80 70 60 50 40 30 20 10 0 -10
f1 (ppm)

^{31}P

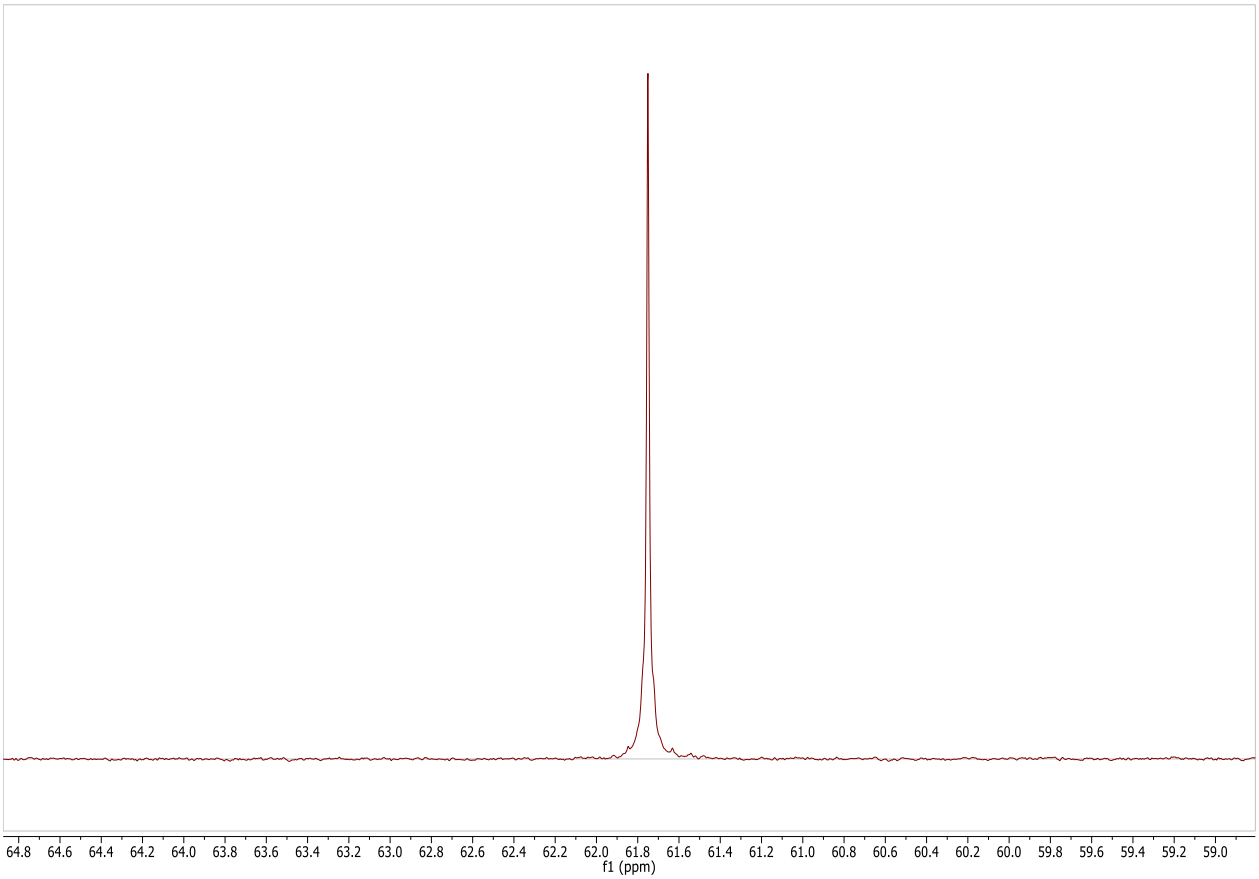
64.8 64.6 64.4 64.2 64.0 63.8 63.6 63.4 63.2 63.0 62.8 62.6 62.4 62.2 62.0 61.8 61.6 61.4 61.2 61.0 60.8 60.6 60.4 60.2 60.0 59.8 59.6 59.4 59.2 59.0
f1 (ppm)